encoding the Gag and Env proteins were much lower than those encoding the Tax and Rex proteins (36). Rex plays an important role in escorting unspliced and incompletely spliced viral mRNAs to the cytoplasm, resulting in enhanced synthesis of viral structural proteins (5, 34, 69). Human CRM1 (hCRM1) is a critical factor for Rex-dependent viral mRNA export to the cytoplasm, and rat CRM1 (rCRM1) cannot substitute for this function (19, 22, 69). Thus, it is reasonable to assume that transgenic (Tg) rats carrying the hCRM1 gene should provide a better environment for HTLV-1 replication and that such animals would provide a better animal model of HTLV-1 infection.

CRM1 is involved in numerous cellular activities, suggesting its essential function in viability, which is supported by the high conservation of CRM1 genes from yeast to humans (37) and by the demonstration that both yeast and mammalian cells defective in CRM1 are inviable (1, 15). In contrast, overexpression of CRM1 has been reported to inhibit early embryogenesis in *Xenopus laevis* (8). Therefore, proper expression of hCRM1 in rats will be essential to produce Tg rats. However, the regulation of CRM1 expression and synthesis has not yet been investigated in detail. Some immortalized cell lines have been reported to maintain CRM1 protein at constant levels throughout the cell cycle, which is compatible with an essential function (37), but other reports have indicated differences in the level of expression of CRM1 among different tissues (28, 37), implying that the expression is regulated. Therefore, we first investigated the expression profile of the CRM1 gene, especially during lymphocyte activation, to determine means for the proper expression of hCRM1 as a transgene. Our results indicate that expression of the CRM1 gene is elaborately regulated during the activation of lymphocytes, including $CD4^+$ T cells, the major targets of HTLV-1. These data suggested that it would be necessary to use a construct harboring the entire regulatory and coding regions of CRM1 for Tg rat construction.

Using a bacterial artificial chromosome (BAC) clone containing the entire CRM1 gene, we have established hCRM1-Tg rats and examined the proliferation of HTLV-1 in vitro and in vivo. Our results demonstrate that T-cell lines isolated from hCRM1-Tg rats produced 100 to 10,000 times more HTLV-1 Gag antigen than T cells from wild-type (Wt) control rats and that Tg rats displayed more-extensive invasion of the thymus by HTLV-1 when infected intraperitoneally. These results indicate the essential role of hCRM1 in proper HTLV-1 replication and suggest the importance of this Tg rat model as a basis for the development of better HTLV-1 animal models.

## MATERIALS AND METHODS

**Cells.** Peripheral blood mononuclear cells (PBMCs) were isolated from healthy donors using Ficoll-Hypaque (Pharmacia) or Ficoll Paque Plus (Amersham Biotechnology) density centrifugation. $CD4^+$ T lymphocytes were purified by negative selection using an immunomagnetic cell sorting apparatus, the MidiMACS cell separator (Miltenyi Biotec), and a cocktail of MACS MicroBeads coupled to hapten-conjugated monoclonal antibodies (MAbs) specific for CD8, CD11b, CD16, CD19, CD36, and CD56. The purity of $CD4^+$ T cells was evaluated by flow cytometry (FACSCalibur; Becton Dickinson) to be approximately 95%.

For activation, cells were cultured with various combinations of 50 nM phorbol 12-myristate 13-acetate (PMA), 100 nM ionomycin, and 10 ng/ml interleukin-2 (IL-2).

The HTLV-1-producing rat and human T-cell lines, FPM1 and MT-2, have been described previously (36, 44). HTLV-1-immortalized cell lines from Wt or Tg rats were established by cocultivating thymocytes or splenocytes with MT-2 cells, which had been treated with mitomycin C (50 μg/ml) for 30 min at 37°C. These cells were maintained in a medium supplemented with 10 U/ml of IL-2 (PeproTech EC) at the beginning of coculture. Some cell lines were eventually freed from exogenous IL-2.

**Western blotting.** Cells were lysed in ice-cold extraction buffer (10 mM Tris-HCl [pH 7.4], 1 mM $MgCl_2$, 0.5% NP-40) containing a protease inhibitor cocktail (Complete Mini; Roche Diagnostics). The protein concentration of each sample was determined using a protein assay kit (QB Perbio; Pierce). The cell lysates were sonicated or, in some cases, treated with DNase 1 solution (Takara) and then dissolved in sample buffer. The same amounts (approximately 20 μg) of cell lysates were subjected to sodium dodecyl sulfate-polyacrylamide gel electrophoresis (SDS-PAGE). Following electrophoresis, proteins were transferred to a nitrocellulose membrane and probed with anti-hCRM1 or anti-rCRM1 (34), anti-β-actin (AC40; Sigma), or anti-Rex (34) antibodies followed by secondary antibodies conjugated to alkaline phosphatase or horseradish peroxidase. Proteins were visualized by staining with 5-bromo-4-chloro-3-indolylphosphate–nitroblue tetrazolium or by ECL+ (Amersham Pharmacia Biotech) followed by the LAS-100 Plus system (Fujifilm) and were evaluated by Image Gauge (version 3.4) software (Fujifilm).

**hCRM1 mRNA quantitative reverse transcription-PCR (RT-PCR).** Total RNA was extracted using the RNeasy Mini kit (QIAGEN) and was treated with RNase-free DNase I (QIAGEN) to minimize contamination of chromosomal DNA. The RNA concentration was measured by absorbance at 260 nm, and purity was ascertained by the ratio of the optical density at 260 nm to that at 280 nm and by gel electrophoresis.

To quantify CRM1 mRNA, RNA samples (5 μg) were subjected to quantitative RT-PCR with the Platinum quantitative RT-PCR Thermoscript one-step system (Invitrogen) using the forward primer 5′-GCT GAA AAC TCA ACC GAG ATG G-3′, the reverse primer 5′-CTG TTG CTC TTG CTG ATG CTG TA-3′, and the probe 6-carboxyfluorescein–AAA ATG CCG CAG GCA TTT CGT TCA G–6-carboxytetramethylrhodamine. RT-PCR was performed by incubation for 2 min at 50°C, 30 min at 60°C, and 10 min at 95°C, followed by 50 cycles of 20 s at 95°C and 1 min at 62°C in an Applied Biosystems Prism 7700 sequence detector thermocycler with Sequence Detector software (Applied Biosystems). To make standard curves, the region from bp −943 to +38 of the CRM1 cDNA was amplified by PCR using Human Lung Marathon-Ready cDNA (Clontech) with adaptor primer 1 and 5′-GCTGCATGGTCTGCTAAC ATT-3′ and by nested PCR with adaptor primer 2 and 5′-CTGCATGGTCTG CTAACATTG-3′. The PCR product was cloned into the pCR 2.1 vector (Invitrogen), and a 981-base single-stranded RNA was synthesized in vitro with MegaScript T7 (Ambion).

**Establishment of hCRM1-Tg rats.** pBeloBAC hCRM1, which harbors the entire hCRM1 genomic sequence including approximately 50 kb of 5′ upstream sequence and 10 kb of 3′ downstream sequence, was microinjected into 450 fertilized 1-cell eggs prepared from Fischer 344/Du Crj female rats by the YS Institute. Integration of the transgene was confirmed by PCR using genomic DNA, extracted with the PUREGENE tissue kit (Gentra) from the rat tail, as a template with the hCRM1-specific primer pairs 5′-TTATGTGGCTGCAGTGT GGA-3′ and 5′-ACATACCAGGGTTCTCTGGA-3′, and 5′-GTCACCTGATG TCGGGAGTT-3′ and 5′-GGATTACAGGTGTGAGCCA-3′. All animal experiments were conducted according to the *Guide for the Care and Use of Laboratory Animals*, Institute for Genetic Medicine, Hokkaido University.

**Detection of genomic copies of hCRM1 and G3PDH.** Genomic DNA was subjected to PCR with the following primer pairs: for hCRM1, forward primer 5′-TGA GGT CAG GAG TTC AGG AT-3′ and reverse primer 5′-CTC TGC CTC CTG GGT TCA A-3′; for glyceraldehyde-3-phosphate dehydrogenase (G3PDH), forward primer 5′-AGA GCT GAA CGG GAA G-3′ and reverse primer 5′-GGA AGA ATG GGA GTT GC-3′. PCR conditions were as follows: 5 min at 94°C; 10 cycles of 30 s at 94°C, 60 s at 69°C, with a decrease of 0.5°C/cycle, and 30 s at 72°C; 8 cycles of 30 s at 94°C, 60 s at 65°C, and 30 s at 72°C; and a final extension for 10 min at 72°C.

**Quantification of HTLV-1 proviral load by LightCycler-based real-time PCR.** The HTLV-1 proviral loads of HTLV-1-infected cells were quantified by real-time PCR on a LightCycler PCR instrument (Roche Diagnostics). Briefly, 20 μl of a PCR mixture in a capillary tube containing each HTLV-1 pX-specific inner primer pair (pX1 and pX4) at 0.4 μM, 1× LightCycler-FastStart SYBR Green PCR master mix, and 30 ng of genomic DNA was subjected to 40 cycles of denaturation (95°C, 15 s), annealing (69°C, 10 s), and extension (72°C, 10 s) following an initial *Taq* polymerase activation step (95°C, 15 min). The copy numbers of HTLV-1 provirus in the samples were estimated from a standard regression curve using LightCycler software, version 3 (Roche Diagnostics). The

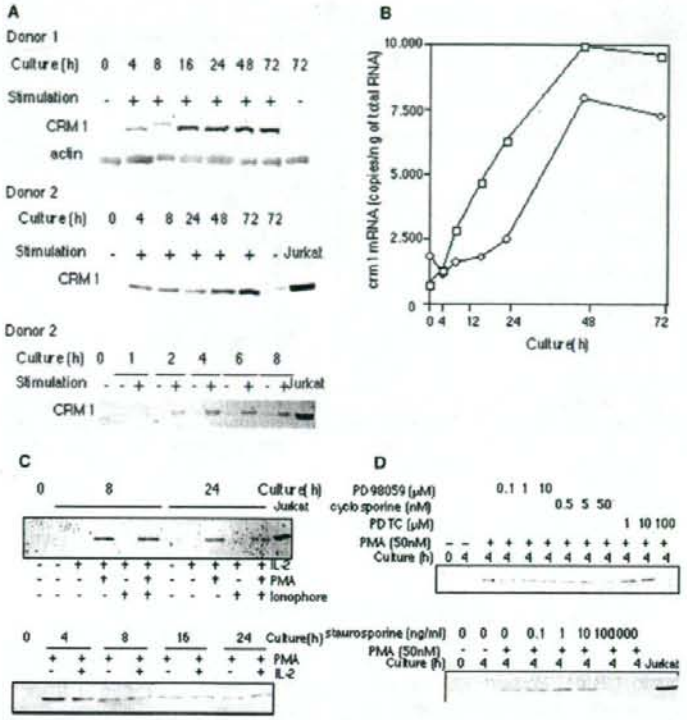


FIG. 1. Expression of CRM1 during activation of PBMCs. (A) PBMCs isolated from donor 1 and donor 2 were activated with ionophore, PMA, and IL-2 and were analyzed by Western blotting. (B) PBMCs isolated from donor 1 (□) and donor 3 (◇) were activated with ionophore, PMA, and IL-2 and were analyzed by quantitative RT-PCR. Each value is the average of duplicate measurements. (C) PBMCs isolated from donor 2 were activated with various combinations of ionophore, PMA, and IL-2 and were analyzed by Western blotting. (D) PBMCs isolated from donor 2 were activated in the presence of various inhibitors and analyzed by Western blotting.

standard curve for HTLV-1 provirus was obtained by PCR data using $1 \times 10^2$ to $1 \times 10^8$ copies of pCR-pX1-4 plasmids, which were constructed by inserting a PCR fragment amplified with pX1 (5′-CCC ACT TCC CAG GGT TTG GAC AGA GTC TTC-3′) and pX4 (5′-GGG GAA GGA GGG GAG TCG AGG GAT AAG GAA-3′) from the genomic DNA of MT-2 cells into pCR2.1. The copy numbers of HTLV-1 provirus were normalized by dividing by the copy numbers of the G3PDH gene in the same samples.

**Detection of HTLV-1 p19.** Each cell line ($10^5$ cells/well) was cultured in 24-well flat-bottom plates for 4 days. The amount of HTLV-1 p19 protein in the culture supernatant or in rat plasma was quantified using an HTLV-1/2 p19 antigen enzyme-linked immunosorbent assay (ZeptoMetrix).

**Detection of intracellular Tax and Gag proteins.** Cells ($10^6$) were fixed with 1% paraformaldehyde in phosphate-buffered saline (PBS) containing 20 μg/ml of lysolecithin (Sigma) for 2 min at room temperature, centrifuged, and resuspended in cold methanol. The cells were then sorted at 4°C for 15 min, centrifuged, and incubated in 0.1% NP-40 in PBS at 4°C for 5 min. After centrifugation, the cells were stained with the mouse anti-Tax MAb LT-4 (63) or the mouse anti-Gag MAb GIN-7 (38), followed by a fluorescein isothiocyanate-conjugated goat antibody against mouse immunoglobulin G (IgG) plus IgM (Immunotech). Finally, the cells were washed and fixed with 1% formalin in PBS prior to analysis by cell sorting.

**Inoculation of HTLV-1 into rats.** Various numbers of mitomycin C-treated or untreated MT-2 cells were intraperitoneally administered to 3- to 6-week-old Wt or hCRM1-Tg rats. Peripheral blood samples were collected from the rats every 2 or 4 weeks after inoculation, and the presence of HTLV-1 provirus in peripheral blood cells and levels of p19 in plasma were determined. In some experiments, rats were euthanized 1 week after inoculation and samples were collected to assess plasma p19 concentrations, proviral loads, and the presence of HTLV-1 provirus.

**Detection of provirus in HTLV-1-infected rats.** To determine the rate of HTLV-1 provirus positivity in various organs, 200 μg of genomic DNA was subjected to PCR for the amplification of the pX region of HTLV-1 as described previously (51). The first-step PCR was performed with the primer pair pX1–pX4, followed by the second-step PCR with the primer pair consisting of pX2 (5′-CGGATACCCAGTCTACGTGTTTGGAGACTGT-3′) and pX3 (5′-GAG CCGATAACGCGTCCATCGATGGGGTCC-3′). PCR conditions were as follows: activation of *Taq* polymerase (94°C, 3 min); 35 cycles of denaturation (94°C, 30 s), annealing (60°C, 30 s), and extension (72°C, 30 s); and a final elongation of the product (72°C, 3 min). For nested PCR, an aliquot of the first PCR product was subjected to another 35 PCR cycles with the second set of primers.

## RESULTS

**Regulated expression of CRM1 in lymphocytes.** We first examined the level of expression of CRM1 mRNA in human tissues by PCR using cDNA derived from the tissues. Expression of CRM1 mRNA was variable in different tissues. Notably, CRM1 mRNA was expressed at very low levels in PBMCs (data not shown). This result was unexpected, because PBMCs include $CD4^+$ T cells, which are the targets of human immunodeficiency virus (HIV) and HTLV-1 (14). Lymphocytes in the PBMC population are mainly in a resting state, leading us to hypothesize that the production of CRM1 is stimulated during lymphocyte activation. Consequently, activated hema-

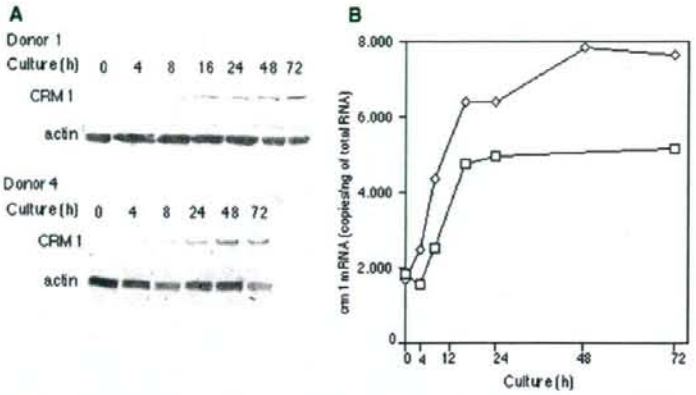


FIG. 2. Time course of CRM1 induction during activation of CD4$^+$ T cells. (A) CD4$^+$ T cells isolated from donor 1 and donor 4 were activated with ionophore, PMA, and IL-2 and were analyzed by Western blotting. (B) Time course of CRM1 mRNA induction during activation of CD4$^+$ T cells. CD4$^+$ T cells isolated from donor 1 (□) and donor 4 (◇) were activated with ionophore, PMA, and IL-2 and were analyzed by quantitative RT-PCR. Each value is the average of duplicate measurements.

topoietic cells should contain CRM1 protein at levels similar to those observed in lymphocyte-derived cell lines. We prepared CD4$^+$ T helper cells, macrophages, and dendritic cells from PBMCs, cultured them in the presence of appropriate cytokines, and compared the amount of CRM1 present in these cells with amounts found in Jurkat cells, a transformed cell line that constitutively expresses CRM1. Western blotting indicated that all activated lymphocyte subsets and monocyte lineage cells expressed CRM1 at levels similar to those in Jurkat cells (data not shown). These results indicate that lymphocyte activation induces high levels of CRM1 expression.

To demonstrate that CRM1 is induced during lymphocyte activation, we stimulated freshly isolated PBMCs with calcium ionophore, PMA, and IL-2, and we examined CRM1 levels at several times by Western blotting (Fig. 1A). The level of CRM1 in resting PBMCs was very low. The CRM1 level clearly increased 4 h after stimulation and then gradually increased further up to 72 h, although some differences were observed between donors 1 and 2. Little change in the level of CRM1 was observed in the absence of stimulation. Actin was used as a loading control, because its level remained relatively constant. These results indicate that the CRM1 gene belongs to the class of early response genes that are induced during lymphocyte activation.

We next measured the levels of CRM1 mRNA by quantitative RT-PCR to determine how the expression of CRM1 is stimulated in PBMCs (Fig. 1B). The amount of CRM1 transcript did increase, but the expression profile differed among individuals. For example, the level of CRM1 mRNA observed in donor 3 was relatively constant up to 24 h after stimulation and then started to increase, while the level of CRM1 mRNA in donor 1 increased gradually over the course of activation. Nevertheless, we consistently found in four experiments that the increase in CRM1 mRNA levels occurred after the increase in CRM1 protein levels. Specifically, up to 4 h after stimulation, marked increases in the level of CRM1 protein were detected, in contrast to nearly constant levels of CRM1 mRNA. Therefore, these results suggest that during lymphocyte activation, CRM1 production is initially stimulated post-transcriptionally and then is further enhanced by upregulating transcription.

In order to identify the signaling pathway responsible for the induction of CRM1 transcription, we activated PBMCs in the presence of various combinations of IL-2, calcium ionophore, and PMA. As shown in Fig. 1C, IL-2 and PMA fully induced CRM1, whereas IL-2 and calcium ionophore did not. Next, we examined whether PMA alone is sufficient to induce CRM1. PMA alone enhanced CRM1 production as efficiently as IL-2 plus PMA. Since PMA is an activator of protein kinase C (PKC) (49), these data suggest that induction of CRM1 is PKC dependent.

To confirm the results described above, we examined the effects of various inhibitors, including staurosporine (a PKC inhibitor) (60) and cyclosporine (a $Ca^{2+}$ cascade inhibitor) (66). As shown in Fig. 1D, staurosporine, but not cyclosporine, inhibited the induction of CRM1, consistent with the results shown in Fig. 1C. We further examined the effects of pyrrolidine dichiocarmate (PDTC) (an NF-κB inhibitor) (43) and PD98059 (a mitogen-activated protein kinase kinase inhibitor) (3) and found that PDTC inhibited CRM1 induction at the highest dose but PD98059 had only a minor effect.

**Regulated expression of CRM1 in CD4$^+$ T lymphocytes.** To examine CRM1 regulation in CD4$^+$ T lymphocytes, resting CD4$^+$ T lymphocytes were purified by negative selection and activated by treatment with a combination of IL-2, ionophore, and PMA. CRM1 levels were estimated by Western blotting (Fig. 2A). CRM1 expression was induced by the same stimuli as in PBMCs, although the kinetics of induction were somewhat different among donors. In contrast to CRM1, the level of actin was constant during T-cell activation. Staurosporine inhibited the enhanced production of CRM1 (data not shown), indicating the involvement of PKC in the induction of CRM1 in CD4$^+$ T cells.

To examine the mechanism underlying the stimulation of CRM1 in CD4$^+$ T cells, we measured the amount of CRM1 mRNA by quantitative RT-PCR (Fig. 2B). As with PBMCs,

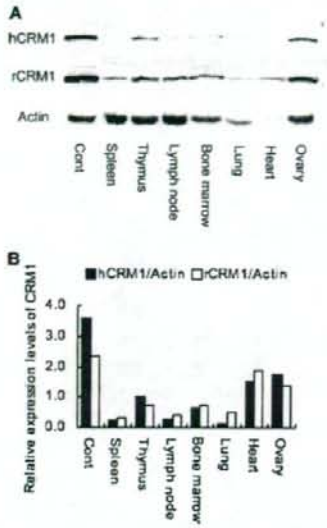


FIG. 3. Tissue distribution of hCRM1 and rCRM1 in hCRM1 Tg rats. (A) Immunoblot assays showing the relative levels of hCRM1 and rCRM1 in rat tissues. Each protein level was determined on immunoblots containing 10 μg of total protein per lane. An FCMT18 cell extract was used as a positive control (Cont). (B) Relative levels of hCRM1 and rCRM1 expression by different organs are shown. Protein expression was quantified by ImageGauge software, and relative values are normalized to the amount of actin.

the amount of CRM1 mRNA also increased during $CD4^+$ T-cell activation. Although the levels of CRM1 mRNA during T-cell activation differed to some extent among donors, similar profiles of induction were observed; after a lag of approximately 4 h, the level of CRM1 mRNA started to increase and continued to do so up to 24 h after stimulation. These results suggest that the increase in CRM1 mRNA is delayed compared to the increase in CRM1 protein, as seen in PBMCs. The level of CRM1 mRNA was constant at times later than 24 h poststimulation, but purified $CD4^+$ T cells appeared unhealthy 2 and 3 days after stimulation in these cultures, as judged by microscopic observation. Therefore, further examination is required to definitively determine the levels of CRM1 protein and mRNA in $CD4^+$ T cells at later times after stimulation.

**Expression of hCRM1 in the Tg rat.** The results described above indicate that regulation of CRM1 expression during the activation of lymphocytes is complex. Considering the lack of characterization of CRM1 regulatory elements, we used a BAC clone, which is likely to harbor the entire regulatory and coding regions of the CRM1 gene, to establish an hCRM1-Tg rat. One rat strain carrying the hCRM1 transgene was obtained from microinjection of the hCRM1-containing BAC clone into 450 fertilized 1-cell eggs from Fischer 344/Du Crj female rats. We assessed the expression of hCRM1 protein in each tissue by immunoblotting using an hCRM1-specific antibody (22). As shown in Fig. 3A, hCRM1 expression was detected in all organs tested. The expression level of this protein was especially high in the ovary and thymus compared to other organs. In addition, expression levels of hCRM1 in the organs were similar to those of endogenous rCRM1 (Fig. 3B). hCRM1 expression was not detected in any organs prepared from Wt rats (data not shown). These data indicate that the Tg rats express hCRM1 in a physiologically relevant manner.

**Enhanced production of $p19^{gag}$ in cell lines derived from Tg rats.** To assess the replication of HTLV-1 in T cells of hCRM1-Tg rats, we established several T-cell lines from both Wt and Tg rats by infecting with HTLV-1. Thymocytes and splenocytes isolated from Wt or hCRM1-Tg rats were cocultured with the HTLV-1-infected human T-cell line MT-2, which had been treated with mitomycin C and then maintained in a culture medium containing 10 U/ml of IL-2. After 2 months of cultivation, we obtained 6 lines from Wt rats and 9 lines from Tg rats (Table 1). As shown in Fig. 4, all of the Tg rat-derived cell lines were confirmed to have the hCRM1 gene (Fig. 4A) and to express hCRM1 (Fig. 4B), whereas none of the Wt rat-derived lines contained the gene or the protein. The expression levels of hCRM1 differed among the cell lines.

We next examined the expression of cell surface markers, including CD3, CD4, CD5, CD8, CD25, major histocompatibility complex class I (MHC-I), and MHC-II, in these cell lines (Table 1). All the cell lines expressed rat CD25 and MHC-I, indicating that they were derived from rat cells, not from the human MT-2 cells. Most of the cell lines also expressed rat CD5 and MHC-II, with the exception of two Wt rat-derived and three Tg rat-derived lines. Expression of rat CD3 was confirmed in six of nine Tg lines, whereas only two of six Wt lines were positive. Rat CD4 expression was detected in one Wt and six Tg cell lines. Rat CD8 was detected in one Wt rat-derived and one Tg rat-derived line. As judged by the expression of CD3, we established a total of eight T-cell lines, two from Wt and six from Tg rats.

We next examined the production of the $p19^{gag}$ protein in the cell lines to assess the effect of hCRM1 on HTLV-1 replication. Our results demonstrated that the Tg rat-derived cell lines produced much greater levels of p19 in the culture supernatant than the Wt rat-derived cells (Fig. 4C). After 2 and 4 days in culture, the mean p19 production by nine Tg rat-

TABLE 1. Constructed cell lines and surface markers

| Cell line | Presence or absence[a] of: | | | | | | | |
|---|---|---|---|---|---|---|---|---|
| | hCRM1 | Surface marker: | | | | | | |
| | | CD3 | CD4 | CD5 | CD8 | CD25 | MHC-I | MHC-II |
| FWT1 | − | + | + | + | − | + | + | + |
| FWS1-11 | − | − | − | + | − | + | + | + |
| FWS1-27 | − | − | − | + | − | + | + | + |
| FWS1-31 | − | − | − | + | (+) | + | + | − |
| FWS1-34 | − | − | − | + | − | + | + | − |
| FWT11 | − | + | − | + | − | + | + | + |
| FCMS1 | + | + | + | + | − | + | + | (+) |
| FCMT1 | + | + | + | + | − | + | + | + |
| FCMT18 | + | + | + | − | − | + | + | − |
| FCMS18 | + | + | + | (+) | − | + | + | (+) |
| FCMT27 | + | + | + | (+) | − | + | + | (+) |
| FCCT13-1 | + | − | − | (+) | − | + | + | + |
| FCCT13-2 | + | + | − | (+) | (+) | + | + | + |
| FCCS13-1 | + | − | − | − | − | + | + | + |
| FCCS13-2 | + | − | (+) | (+) | − | + | + | − |

[a] +, positive; (+), weakly positive; −, negative.

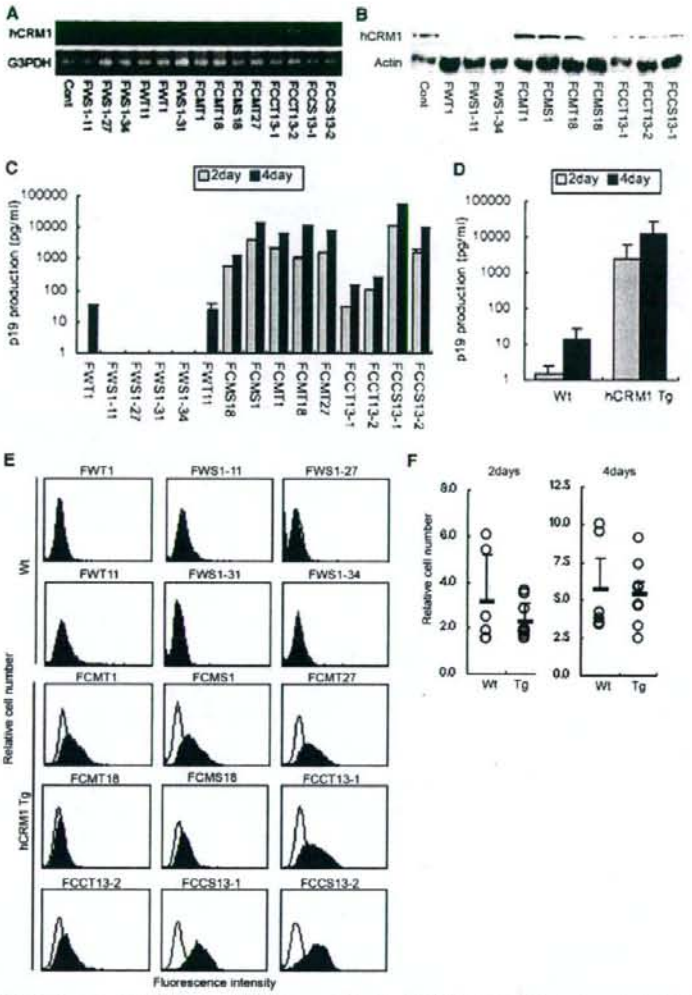


FIG. 4. Expression of HTLV-1 Gag and hCRM1 in cell lines immortalized with HTLV-1. (A) Detection of the hCRM1 transgene in cell lines by PCR. DNA extracted from each cell line (100 ng) was subjected to PCR with primers for hCRM1 and with primers for G3PDH as an internal control. (B) Protein expression of hCRM1 was detected by immunoblotting. Samples (10 μg of total protein per lane) were subjected to SDS-PAGE. A HeLa cell extract was used as a positive control (Cont). (C) HTLV-1 Gag protein levels in the supernatants of 2-day and 4-day cultures were quantified by an HTLV-1 p19 enzyme-linked immunosorbent assay. Results are means from three independent experiments. (D) Based on the data shown in panel C, the average $p19^{gag}$ production of Tg and Wt cell lines was calculated. (E) The amount of intracellular Gag in each cell line was analyzed by flow cytometry. Open histograms, cells stained with MAbs against $p19^{gag}$ and $p55^{gag}$; solid histograms, cells stained with control mouse IgG. (F) The growth rates of Wt and Tg cell lines were measured. In parallel with the experiments described in the legend to panel C, the growth rate was monitored by the cell-counting Kit-8 (Dojinndo Laboratories). The relative numbers of cells in 2- or 4-day cultures versus day zero cultures are shown.

derived cell lines was 1,000 ± 10 and 10,000 ± 100 times higher, respectively, than the mean production of the six Wt rat-derived lines (Fig. 4D). The amounts (1 to 60 ng/ml) of p19 released from the Tg rat-derived cell lines are equivalent to those from human HTLV-1-producing T-cell lines, such as MT-2 and MT-4 (data not shown). These results clearly demonstrate the enhanced production of the HTLV-1 Gag protein in the cells expressing hCRM1.

To further examine the increased p19 production in each cell line expressing hCRM1, we conducted a fluorescence-activated cell sorter analysis to detect the intracellular Gag protein. As shown in Fig. 4E, we were able to detect p19 and the precursor $p55^{gag}$ protein in all cell lines derived from Tg rats. In contrast, no Wt rat-derived cell lines produced detectable amounts of Gag. These results further support the role of hCRM1 in the enhancement of HTLV-1 Gag production.

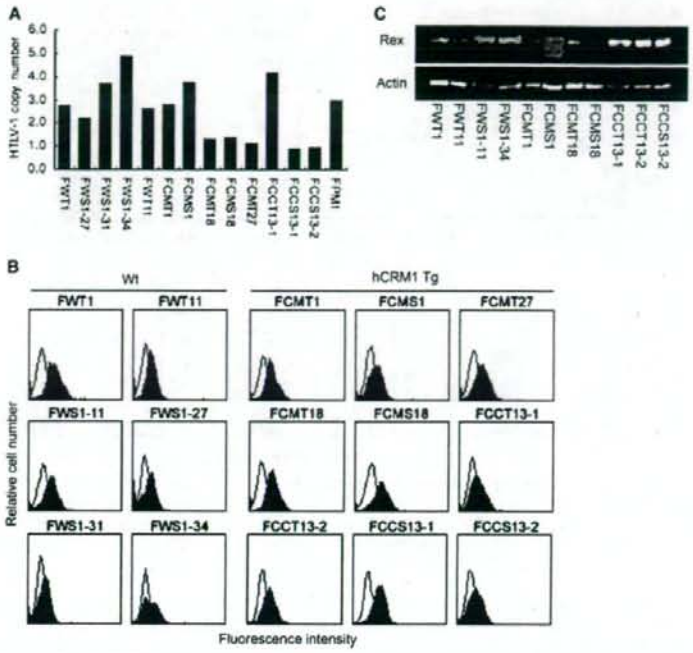


FIG. 5. Viral loads and expression in HTLV-1-transformed T cells derived from Tg and Wt rats. (A) The proviral load of each cell line was measured by quantitative real-time PCR. The copy number of HTLV-1 provirus was normalized by dividing by the G3PDH copy number in the same sample. (B) The production of intracellular Tax in each cell line was analyzed by flow cytometry. Solid histograms, cells stained with an anti-Tax MAb; open histograms, cells stained with control mouse IgG. (C) The Rex expression of each cell line was detected by immunoblotting. Ten micrograms of total protein per lane was subjected to SDS-PAGE. Lower bands in FCMS1 and FCMS18 samples represent $p21^{rex}$.

We also assessed the proliferation of each cell line to exclude the possibility that the enhanced production was not due to increased production by individual cells but was the result of increases in the number of cells in the Tg rat-derived lines. As shown in Fig. 4F, we confirmed that there was no difference in the proliferation rate between Wt rat-derived and Tg rat-derived cell lines after 2 or 4 days in culture. In addition, there was no correlation between the rate of cell growth and the amount of p19 in the culture in any cell line.

**The state of HTLV-1 infection is not correlated with levels of p19 production.** We also assessed the proviral load of each cell line to rule out the possibility that enhanced production of Gag was due to increased provirus copy numbers in Tg cell lines. Real-time PCR analysis using a pair of primers for the Tax gene was performed to quantify the number of integrated provirus copies. As a relative standard, we used genomic DNA from FPM1 cells, which contain 3 copies of HTLV-1 provirus per cell (36). As shown in Fig. 5A, all five Wt cell lines contained more than 2 copies of the provirus, whereas most of the Tg lines appeared to have only 1 provirus copy per cell, with the exception of FCCT13-1 cells, which possessed 4 copies. Thus, there was no correlation between the provirus copy number and p19 production, indicating that differences in the amount of provirus were not responsible for the enhanced Gag production in Tg rat-derived cells.

Altered expression of Tax and Rex could also be associated with enhanced expression of Gag in Tg rat-derived cells. Thus, we investigated the expression of Tax in the cell lines. As shown in Fig. 5B, fluorescence-activated cell sorter analysis revealed that all of the cell lines tested expressed detectable levels of Tax proteins. Although we observed differences in the levels of Tax expression among the cell lines, there was no significant difference in Tax expression between Wt rat- and Tg rat-derived lines.

We next examined Rex expression by immunoblotting. As shown in Fig. 5C, the Rex protein was expressed in all cell lines tested. Again, there was no statistical difference in Rex protein expression between Wt and Tg cells. Two Tg cell lines, FCMS1 and FCMS18, expressed p21 protein as well as $p27^{rex}$. This expression was not associated with elevated expression of Gag, since the amounts of $p19^{gag}$ produced by these two cell lines were similar to those for the other Tg rat-derived cell lines (Fig. 4C and D). These results indicate that the number of integrated provirus copies and the expression levels of Tax and Rex are not correlated with the enhanced expression of Gag observed in cell lines derived from hCRM1-Tg rats.

**Enhanced dissemination of HTLV-1 in hCRM1-Tg rats.** We next examined the proliferation of HTLV-1 in Tg rats by inoculating animals with the HTLV-1-producing human T-cell line MT-2 as a virus source. Analysis of plasma p19 concentrations in the infected rats over time did not show significant differences between Tg and Wt rats, although p19 concentra-

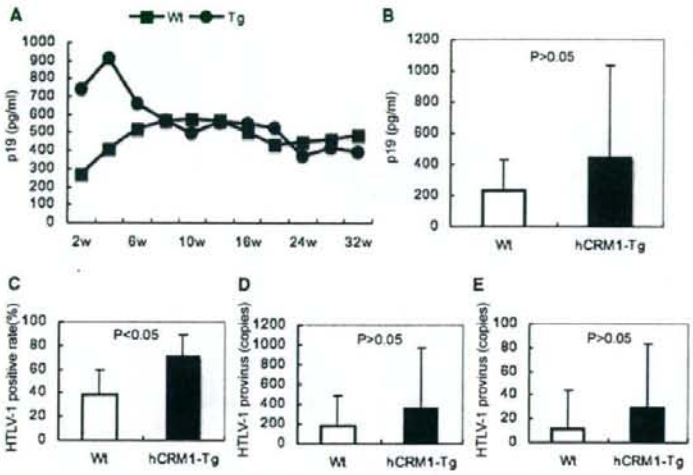


FIG. 6. Dissemination of HTLV-1 in hCRM1-Tg rats. (A) Mean plasma p19 concentration in Wt ($n$ = 9) or hCRM1-Tg ($n$ = 7) rats after intraperitoneal inoculation of mitomycin C-treated MT-2 cells ($1 \times 10^7$ per animal). (B) Mean plasma p19 concentration in Wt ($n$ = 16) or hCRM1-Tg ($n$ = 17) rats 1 week after intraperitoneal inoculation of MT-2 cells ($5 \times 10^6$ per animal). (C) Detection of the HTLV-1 provirus in thymuses derived from rats used for the experiment for which results are shown in panel B. The presence of the HTLV-1 provirus was analyzed by nested PCR. Results are mean percentages of HTLV-1 provirus-positive rats from five independent experiments. (D and E) HTLV-1 proviral loads of rats used in the experiment for which results are shown in panel B. HTLV-1 proviral loads in peripheral blood cells (D) or thymuses (E) were quantified by real-time PCR. The relative copy numbers of HTLV-1 provirus per $2 \times 10^7$ copies of G3PDH are shown. Results are expressed as means + standard deviations. The statistical significance of differences, shown in panels B to E, was determined by Student's $t$ test, using Microsoft Excel 2004 software for Mac.

tions in Tg rats tended to be higher during the first 6 weeks after infection (Fig. 6A). Figure 6B shows the mean plasma p19 concentration in rats after 1 week of infection and again demonstrates higher, but not significantly different, levels of the viral protein in Tg rat-derived samples. To evaluate the dissemination of the virus in vivo, we determined the presence of HTLV-1 provirus DNA in various organs 1 week after intraperitoneal infection by a nested PCR that specifically amplifies a part of the px region. We calculated the percentage of rats that sustained the px gene in five independent experiments and found that the rate at which the virus disseminated to the thymus in Tg rats was significantly higher than that for Wt rats (Fig. 6C). However, we have not detected notable differences between the two groups in HTLV-1 proviral loads in various organs, including peripheral blood cells and the thymus (Fig. 6D and E; also data not shown). These results indicate the limited effects of hCRM1 on the proliferation of HTLV-1 in vivo, in dramatic contrast to the significant enhancement of HTLV-1 production in Tg rat-derived cells in vitro.

## DISCUSSION

Unlike hCRM1, rCRM1 does not support Rex function, due to its inability to induce Rex-Rex dimerization, which is required for RNA export from the nucleus to the cytoplasm (22). This may be one reason why HTLV-1 replicates poorly in rats compared to humans. This observation suggests that the hCRM1-Tg rats would be novel animal models, since they would support better replication of HTLV-1.

The essential role of CRM1 in cell viability suggested that proper expression of the transgene would be key for the successful construction of Tg rats. Therefore, we examined the expression pattern of CRM1 and found that CRM1 is expressed in a manner similar to that of the early response genes induced during the activation of lymphocytes, including $CD4^+$ T cells. Our results suggest that expression of CRM1 is stimulated in two steps: in the first phase, lasting approximately 4 h, induction is regulated primarily in a posttranscriptional manner, and in the second phase, transcriptional augmentation takes place. Alternatively, CRM1 protein in PBMCs may be rapidly turned over and then protected from degradation upon stimulation, giving rise to the early increase in protein levels. The profile of CRM1 expression further suggests that the initial induction occurs in the $G_1$ phase of the cell cycle, a hypothesis also supported by the observation that mimosine, which blocks the cell cycle in late $G_1$ (65), does not prevent the induction (data not shown).

The elaborate regulation of CRM1 expression led us to use a BAC clone harboring the entire hCRM1 gene for Tg rat construction. An initial unsuccessful trial using the mouse H2 promoter to express hCRM1 cDNA supports the necessity of using the hCRM1 BAC. Our results indicate that the hCRM1 BAC Tg rats express hCRM1 in various organs, including the thymus and spleen, in a manner similar to expression of endogenous rCRM1 in rats. Moreover, the distribution of hCRM1 in the Tg rats is similar to that observed in humans (28, 37). Therefore, use of the hCRM1 BAC construct may have resulted in physiological expression of the protein in Tg rats. We also demonstrated hCRM1 expression in all Tg rat-derived cell lines, which will be useful for the functional analysis of hCRM1 in HTLV-1-infected cells.

We have previously reported that expression of hCRM1 induced an increase in HTLV-1 Gag production in both rat epithelial and T cells (21, 69). Our present study also showed that T-cell lines established from hCRM1-Tg rats produced significantly greater amounts of p19 than cell lines established from Wt rats, further indicating the positive effect of hCRM1 on viral protein synthesis. This effect was not due to the effects of Tax or Rex proteins, which enhance the transcription of total viral mRNAs and the nuclear export of unspliced and incompletely spliced mRNAs, respectively (12, 26, 30, 68), since the expression levels of these proteins were not significantly different in the Tg and Wt cell lines. Additionally, these results indicate that induction of hCRM1 expression does not affect the expression of HTLV-1 regulatory proteins in virus-infected rat cells. We also observed differences in the levels of p19 production among the cell lines derived from hCRM1-Tg rats. Since the amount of p19 did not correlate with the expression level of hCRM1, Tax, or Rex, the reason for the differences is not clear. Some other factors, including RanGTP and RanBP3, which play important roles in the nuclear export of CRM1-substrate complexes (14, 41, 47, 59), may affect the levels of p19 production in the rat cell lines. It is also possible that the integration sites of the provirus influence virus production. Further studies are required to identify the factors that result in different p19 production among Tg rat-derived cell lines.

Differences in the expression of cell surface proteins were also observed among the cell lines established (Table 1). It is especially interesting that most of the Wt rat-derived cells do not express CD3 or CD4, whereas the majority of the Tg rat-derived lines possess both of these molecules. Since we and others have established a number of CD4-positive cell lines from various strains of Wt rats (31, 36), the present results may be due to experimental disparities. However, it is possible that enhanced HTLV-1 production by the hCRM1-expressing cells and subsequent dissemination of the virus in the culture may influence the phenotypes of the transformed cells. Thus, additional studies are required to determine the significance and cause of the difference.

The Tg rats showed minimal effects on HTLV-1 replication in vivo. Since dramatic enhancement of HTLV-1 production was observed in all hCRM1-expressing cells in vitro, it is possible that the number of HTLV-1-infected cells in vivo was too low to detect differences in virus production between Wt and Tg rats. From this point of view, alteration of experimental conditions to improve the initial HTLV-1 infection rate may lead to enhanced viral replication in Tg rats. Repression of viral protein expression in vivo may also reduce the effects of hCRM1, masking the enhanced viral replication in Tg rats. Such responses have been well documented for HTLV-1-infected individuals (32, 33). It is also possible that HTLV-1-specific immune responses could affect the replication of HTLV-1 in the Tg rats. Indeed. Our preliminary experiments indicated that induction of HTLV-1-specific cytotoxic T-lymphocyte responses occurred as early as 1 week after virus infection. Alternatively, some other host factors may govern and modulate efficient HTLV-1 replication in vivo. Thus, further studies on both virological and immunological aspects are required to verify the importance of the Tg rats as an in vivo model of HTLV-1 infection.

The HTLV-1 Rex protein is able to functionally replace the Rev protein of HIV type 1 (HIV-1) (57). CRM1 is a nuclear export factor for HIV-1 Rev, and a truncated Rev mutant with weakened binding affinity to CRM1 results in reduced levels of HIV-1 Gag production (20). These results raise the possibility that rat cells expressing hCRM1 protein can produce enhanced levels of HIV-1 structural proteins. Indeed, our preliminary results demonstrate that hCRM1 promotes HIV-1 $p24^{gag}$ production in rat cells (unpublished data). Thus, the hCRM1-Tg rats generated in this study may also be useful as a small-animal model of HIV-1 infection, when HIV-1 receptors are simultaneously expressed in these rats.

HIV latently infects reservoirs of resting T cells (7, 9, 10, 13, 61), which are thought to be in the $G_0$ state, and the virus is then reactivated during T-cell activation. Alternatively, HIV has also been reported to propagate efficiently in nonreplicating lymphatic T cells (18), which lack certain markers specific for activation. Since cytokine levels are high in lymphatic tissues, the progression of T cells from $G_0$ to $G_1$ may support HIV replication. Although release from the cell cycle block has been extensively investigated at the transcriptional level, a recent study has shown that the synthesis of unspliced HIV Gag RNA increases rapidly during the HIV reactivation process, to a much greater extent than the synthesis of multiply spliced RNAs (7). Our results demonstrating a rapid increase in CRM1 expression during lymphocyte activation provide a clue to the underlying mechanism, the efficient action of the HIV Rev protein, which leads to robust synthesis of unspliced RNA. We suggest that HIV gene expression is regulated in lymphocytes at both the transcriptional and RNA export levels.

Independently of viral replication, the first phase of enhancement of CRM1 expression is also coincident with the induction of cytokines, such as IL-2 (4). CRM1 interacts with the AU-rich element (ARE) located in the 3′ untranslated region of c-*fos* mRNA (via HuR and its ligands) and mediates export of this mRNA from the nucleus to the cytoplasm (6, 16). Therefore, CRM1 may transport cytokine mRNAs belonging to the early response genes, since many cytokine mRNAs harbor ARE sequences (24, 56). Collectively, these observations suggest that enhancement of mRNA export via the induction of CRM1 expression, in addition to regulation at the transcriptional and translational levels, may play an important role in coordinating gene expression during lymphocyte activation. The existence of a posttranscriptional mechanism leading to a rapid increase in CRM1 protein levels is consistent with this hypothesis.

In conclusion, we have established a novel Tg rat carrying the hCRM1 gene via examination of the expression of this gene, and we have isolated several HTLV-1-infected T-cell lines expressing hCRM1. Our results demonstrate that T cells from hCRM1-Tg rats produced enhanced levels of the HTLV-1 Gag protein compared to T cells from Wt control rats. These results indicate the essential role of hCRM1 in proper HTLV-1 replication and suggest the importance of this Tg rat in the development of HTLV-1 animal models. These animals may also contribute to the development of models for other human retroviruses, such as HIV-1.

## ACKNOWLEDGMENTS

Buffy coats for the isolation of lymphocytes were the kind gift of the Hokkaido Red Cross Blood Center (Sapporo, Japan). We thank A. Hirano, N. Mizuno, K. Nakajima, and J. Hioki for excellent technical assistance.

This study was supported by grants from the Ministry of Sports and Culture (Japan) and the Ministry of Health and Welfare (Japan).

## REFERENCES

1. **Adachi, Y., and M. Yanagida.** 1989. Higher order chromosome structure is affected by cold-sensitive mutations in a *Schizosaccharomyces pombe* gene CRM1+ which encodes a 115-kD protein preferentially localized in the nucleus and its periphery. J. Cell Biol. **108:**1195–1207.
2. **Akagi, T., I. Takeda, T. Oka, Y. Ohtsuki, S. Yano, and I. Miyoshi.** 1985. Experimental infection of rabbits with human T-cell leukemia virus type I. Jpn. J. Cancer Res. **76:**86–94.
3. **Alessi, D. R., A. Cuenda, P. Cohen, D. T. Dudley, and A. R. Saltiel.** 1995. PD 098059 is a specific inhibitor of the activation of mitogen-activated protein kinase kinase in vitro and in vivo. J. Biol. Chem. **270:**27489–27494.
4. **Ashwell, J. D., and R. D. Klusner.** 1990. Genetic and mutational analysis of the T-cell antigen receptor. Annu. Rev. Immunol. **8:**139–167.
5. **Bogerd, H. P., R. A. Fridell, R. E. Benson, J. Hua, and B. R. Cullen.** 1996. Protein sequence requirements for function of the human T-cell leukemia virus type 1 Rex nuclear export signal delineated by a novel in vivo randomization-selection assay. Mol. Cell. Biol. **16:**4207–4214.
6. **Brennan, C. M., I. E. Gallouzi, and J. A. Steitz.** 2000. Protein ligands to HuR modulate its interaction with target mRNAs in vivo. J. Cell Biol. **151:**1–14.
7. **Brooks, D. G., S. G. Kitchen, C. M. Kitchen, D. D. Scripture-Adams, and J. A. Zack.** 2001. Generation of HIV latency during thymopoiesis. Nat. Med. **7:**459–464.
8. **Callanan, M., N. Kudo, S. Gout, M. Brocard, M. Yoshida, S. Dimitrov, and S. Khochbin.** 2000. Developmentally regulated activity of CRM1/XPO1 during early *Xenopus* embryogenesis. J. Cell Sci. **113:**451–459.
9. **Chun, T. W., D. Engel, M. M. Berrey, T. Shea, L. Corey, and A. S. Fauci.** 1998. Early establishment of a pool of latently infected, resting CD4+ T cells during primary HIV-1 infection. Proc. Natl. Acad. Sci. USA **95:**8869–8873.
10. **Chun, T. W., L. Stuyver, S. B. Mizell, L. A. Ehler, J. A. Mican, M. Baseler, A. L. Lloyd, M. A. Nowak, and A. S. Fauci.** 1997. Presence of an inducible HIV-1 latent reservoir during highly active antiretroviral therapy. Proc. Natl. Acad. Sci. USA **94:**13193–13197.
11. **Daenke, S., S. Nightingale, J. K. Cruickshank, and C. R. Bangham.** 1990. Sequence variants of human T-cell lymphotropic virus type I from patients with tropical spastic paraparesis and adult T-cell leukemia do not distinguish neurological from leukemic isolates. J. Virol. **64:**1278–1282.
12. **Fang, J., S. Kushida, R. Feng, M. Tanaka, T. Kawamura, H. Abe, N. Maeda, M. Onobori, M. Hori, K. Uchida, and M. Miwa.** 1998. Transmission of human T-cell leukemia virus type 1 to mice. J. Virol. **72:**3952–3957.
13. **Finzi, D., M. Hermankova, T. Pierson, L. M. Carruth, C. Buck, R. E. Chaisson, T. C. Quinn, K. Chadwick, J. Margolick, R. Brookmeyer, J. Gallant, M. Markowitz, D. D. Ho, D. D. Richman, and R. F. Siliciano.** 1997. Identification of a reservoir for HIV-1 in patients on highly active antiretroviral therapy. Science **278:**1295–1300.
14. **Fornerod, M., M. Ohno, M. Yoshida, and I. W. Mattaj.** 1997. CRM1 is an export receptor for leucine-rich nuclear export signals. Cell **90:**1051–1060.
15. **Fornerod, M., J. van Deursen, S. van Baal, A. Reynolds, D. Davis, K. G. Murti, J. Fransen, and G. Grosveld.** 1997. The human homologue of yeast CRM1 is in a dynamic subcomplex with CAN/Nup214 and a novel nuclear pore component Nup88. EMBO J. **16:**807–816.
16. **Gallouzi, I. E., and J. A. Steitz.** 2001. Delineation of mRNA export pathways by the use of cell-permeable peptides. Science **294:**1895–1901.
17. **Gessain, A., F. Barin, J. C. Vernant, O. Gout, L. Maurs, A. Calender, and G. de The.** 1985. Antibodies to human T-lymphotropic virus type-I in patients with tropical spastic paraparesis. Lancet **ii:**407–410.
18. **Haase, A. T., K. Henry, M. Zupancic, G. Sedgewick, R. A. Faust, H. Melroe, W. Cavert, K. Gebhard, K. Staskus, Z. Q. Zhang, P. J. Dailey, H. H. Balfour, Jr., A. Erice, and A. S. Perelson.** 1996. Quantitative image analysis of HIV-1 infection in lymphoid tissue. Science **274:**985–989.
19. **Hakata, Y., T. Umemoto, S. Matsushita, and H. Shida.** 1998. Involvement of human CRM1 (exportin 1) in the export and multimerization of the Rex protein of human T-cell leukemia virus type 1. J. Virol. **72:**6602–6607.
20. **Hakata, Y., M. Yamada, N. Mabuchi, and H. Shida.** 2002. The carboxy-terminal region of the human immunodeficiency virus type 1 protein Rev has multiple roles in mediating CRM1-related Rev functions. J. Virol. **76:**8079–8089.
21. **Hakata, Y., M. Yamada, and H. Shida.** 2003. A multifunctional domain in human CRM1 (exportin 1) mediates RanBP3 binding and multimerization of human T-cell leukemia virus type 1 Rex protein. Mol. Cell. Biol. **23:**8751–8761.
22. **Hakata, Y., M. Yamada, and H. Shida.** 2001. Rat CRM1 is responsible for the poor activity of human T-cell leukemia virus type 1 Rex protein in rat cells. J. Virol. **75:**11515–11525.
23. **Hall, W. W., C. R. Liu, O. Schneewind, H. Takahashi, M. H. Kaplan, G. Roupe, and A. Vahlne.** 1991. Deleted HTLV-I provirus in blood and cutaneous lesions of patients with mycosis fungoides. Science **253:**317–320.
24. **Hamilton, T. A., Y. Ohmori, and J. Tebo.** 2002. Regulation of chemokine expression by antiinflammatory cytokines. Immunol. Res. **25:**229–245.
25. **Hanabuchi, S., T. Ohashi, Y. Koya, H. Kato, A. Hasegawa, F. Takemura, T. Masuda, and M. Kannagi.** 2001. Regression of human T-cell leukemia virus type I (HTLV-I)-associated lymphomas in a rat model: peptide-induced T-cell immunity. J. Natl. Cancer Inst. **93:**1775–1783.
26. **Hidaka, M., J. Inoue, M. Yoshida, and M. Seiki.** 1988. Post-transcriptional regulator (rex) of HTLV-1 initiates expression of viral structural proteins but suppresses expression of regulatory proteins. EMBO J. **7:**519–523.
27. **Hinuma, Y., K. Nagata, M. Hanaoka, M. Nakai, T. Matsumoto, K. I. Kinoshita, S. Shirakawa, and I. Miyoshi.** 1981. Adult T-cell leukemia: antigen in an ATL cell line and detection of antibodies to the antigen in human sera. Proc. Natl. Acad. Sci. USA **78:**6476–6480.
28. **Holaska, J. M., and B. M. Paschal.** 1998. A cytosolic activity distinct from CRM1 mediates nuclear export of protein kinase inhibitor in permeabilized cells. Proc. Natl. Acad. Sci. USA **95:**14739–14744.
29. **Hoshino, H., H. Tanaka, K. Shimotohno, M. Miwa, M. Nagai, M. Shimoyama, and T. Sugimura.** 1984. Immortalization of peripheral blood lymphocytes of cats by human T-cell leukemia virus. Int. J. Cancer **34:**513–517.
30. **Inoue, J., M. Yoshida, and M. Seiki.** 1987. Transcriptional (p40x) and post-transcriptional (p27x-III) regulators are required for the expression and replication of human T-cell leukemia virus type I genes. Proc. Natl. Acad. Sci. USA **84:**3653–3657.
31. **Ishiguro, N., M. Abe, K. Seto, H. Sakurai, H. Ikeda, A. Wakisaka, T. Togashi, M. Tateno, and T. Yoshiki.** 1992. A rat model of human T lymphocyte virus type I (HTLV-I) infection. 1. Humoral antibody response, provirus integration, and HTLV-I-associated myelopathy/tropical spastic paraparesis-like myelopathy in seronegative HTLV-I carrier rats. J. Exp. Med. **176:**981–989.
32. **Kannagi, M., S. Matsushita, and S. Harada.** 1993. Expression of the target antigen for cytotoxic T lymphocytes on adult T-cell-leukemia cells. Int. J. Cancer **54:**582–588.
33. **Kannagi, M., K. Sugamura, K. Kinoshita, H. Uchino, and Y. Hinuma.** 1984. Specific cytolysis of fresh tumor cells by an autologous killer T cell line derived from an adult T cell leukemia/lymphoma patient. J. Immunol. **133:**1037–1041.
34. **Kim, F. J., A. A. Beeche, J. J. Hunter, D. J. Chin, and T. J. Hope.** 1996. Characterization of the nuclear export signal of human T-cell lymphotropic virus type 1 Rex reveals that nuclear export is mediated by position-variable hydrophobic interactions. Mol. Cell. Biol. **16:**5147–5155.
35. **Kinoshita, T., A. Tsujimoto, and K. Shimotohno.** 1991. Sequence variations in LTR and env regions of HTLV-I do not discriminate between the virus from patients with HTLV-I-associated myelopathy and adult T-cell leukemia. Int. J. Cancer **47:**491–495.
36. **Koya, Y., T. Ohashi, H. Kato, S. Hanabuchi, T. Tsukahara, F. Takemura, K. Etoh, M. Matsuoka, M. Fujii, and M. Kannagi.** 1999. Establishment of a seronegative human T-cell leukemia virus type 1 (HTLV-1) carrier state in rats inoculated with a syngeneic HTLV-1-immortalized T-cell line preferentially expressing Tax. J. Virol. **73:**6436–6443.
37. **Kudo, N., S. Khochbin, K. Nishi, K. Kitano, M. Yanagida, M. Yoshida, and S. Horinouchi.** 1997. Molecular cloning and cell cycle-dependent expression of mammalian CRM1, a protein involved in nuclear export of proteins. J. Biol. Chem. **272:**29742–29751.
38. **Kurihara, K., N. Harashima, S. Hanabuchi, M. Masuda, A. Utsunomiya, R. Tanosaki, M. Tomonaga, T. Ohashi, A. Hasegawa, T. Masuda, J. Okamura, Y. Tanaka, and M. Kannagi.** 2005. Potential immunogenicity of adult T cell leukemia cells in vivo. Int. J. Cancer **114:**257–267.
39. **Kushida, S., H. Mizusawa, M. Matsumura, H. Tanaka, Y. Ami, M. Hori, K. Yagami, T. Kameyama, Y. Tanaka, A. Yoshida, H. Nyunoya, K. Shimotohno, Y. Iwasaki, K. Uchida, and M. Miwa.** 1994. High incidence of HAM/TSP-like symptoms in WKA rats after administration of human T-cell leukemia virus type 1-producing cells. J. Virol. **68:**7221–7226.
40. **LaGrenade, L., B. Hanchard, V. Fletcher, B. Cranston, and W. Blattner.** 1990. Infective dermatitis of Jamaican children: a marker for HTLV-I infection. Lancet **336:**1345–1347.
41. **Lindsay, M. E., J. M. Holaska, K. Welch, B. M. Paschal, and I. G. Macara.** 2001. Ran-binding protein 3 is a cofactor for CRM1-mediated nuclear protein export. J. Cell Biol. **153:**1391–1402.
42. **Mann, D. L., P. DeSantis, G. Mark, A. Pfeifer, M. Newman, N. Gibbs, M. Popovic, M. G. Sarngadharan, R. C. Gallo, J. Clark, and W. Blattner.** 1987. HTLV-I–associated B-cell CLL: indirect role for retrovirus in leukemogenesis. Science **236:**1103–1106.
43. **Martinez-Martinez, S., P. Gomez del Arco, A. L. Armesilla, J. Aramburu, C. Luo, A. Rao, and J. M. Redondo.** 1997. Blockade of T-cell activation by dithiocarbamates involves novel mechanisms of inhibition of nuclear factor of activated T cells. Mol. Cell. Biol. **17:**6437–6447.
44. **Miyoshi, I., I. Kubonishi, S. Yoshimoto, T. Akagi, Y. Ohtsuki, Y. Shiraishi, K. Nagata, and Y. Hinuma.** 1981. Type C virus particles in a cord T-cell line

derived by co-cultivating normal human cord leukocytes and human leukaemic T cells. Nature **294:**770–771.

45. **Nakamura, H., M. Hayami, Y. Ohta, K. Ishikawa, H. Tsujimoto, T. Kiyokawa, M. Yoshida, A. Sasagawa, and S. Honjo.** 1987. Protection of cynomolgus monkeys against infection by human T-cell leukemia virus type-I by immunization with viral *env* gene products produced in *Escherichia coli*. Int. J. Cancer **40:**403–407.
46. **Nakamura, H., Y. Tanaka, A. Komuro-Tsujimoto, K. Ishikawa, K. Takadaya, H. Tozawa, H. Tsujimoto, S. Honjo, and M. Hayami.** 1986. Experimental inoculation of monkeys with autologous lymphoid cell lines immortalized by and producing human T-cell leukemia virus type-I. Int. J. Cancer **38:**867–875.
47. **Nemergut, M. E., M. E. Lindsay, A. M. Brownawell, and I. G. Macara.** 2002. Ran-binding protein 3 links CRM1 to the Ran guanine nucleotide exchange factor. J. Biol. Chem. **277:**17385–17388.
48. **Nishioka, K., I. Maruyama, K. Sato, I. Kitajima, Y. Nakajima, and M. Osame.** 1989. Chronic inflammatory arthropathy associated with HTLV-I. Lancet **i:**441.
49. **Nishizuka, Y.** 1984. The role of protein kinase C in cell surface signal transduction and tumour promotion. Nature **308:**693–698.
50. **Nomura, M., T. Ohashi, K. Nishikawa, H. Nishitsuji, K. Kurihara, A. Hasegawa, R. A. Furuta, J. Fujisawa, Y. Tanaka, S. Hanabuchi, N. Harashima, T. Masuda, and M. Kannagi.** 2004. Repression of Tax expression is associated both with resistance of human T-cell leukemia virus type 1-infected T cells to killing by Tax-specific cytotoxic T lymphocytes and with impaired tumorigenicity in a rat model. J. Virol. **78:**3827–3836.
51. **Ohashi, T., S. Hanabuchi, H. Kato, Y. Koya, F. Takemura, K. Hirokawa, T. Yoshiki, Y. Tanaka, M. Fujii, and M. Kannagi.** 1999. Induction of adult T-cell leukemia-like lymphoproliferative disease and its inhibition by adoptive immunotherapy in T-cell-deficient nude rats inoculated with syngeneic human T-cell leukemia virus type 1-immortalized cells. J. Virol. **73:**6031–6040.
52. **Ohashi, T., S. Hanabuchi, H. Kato, H. Tateno, F. Takemura, T. Tsukahara, Y. Koya, A. Hasegawa, T. Masuda, and M. Kannagi.** 2000. Prevention of adult T-cell leukemia-like lymphoproliferative disease in rats by adoptively transferred T cells from a donor immunized with human T-cell leukemia virus type 1 Tax-coding DNA vaccine. J. Virol. **74:**9610–9616.
53. **Oka, T., H. Sonobe, J. Iwata, I. Kubonishi, H. Satoh, M. Takata, Y. Tanaka, M. Tateno, H. Tozawa, S. Mori, T. Yoshiki, and Y. Ohtsuki.** 1992. Phenotypic progression of a rat lymphoid cell line immortalized by human T-lymphotropic virus type I to induce lymphoma/leukemia-like disease in rats. J. Virol. **66:**6686–6694.
54. **Osame, M., K. Usuku, S. Izumo, N. Ijichi, H. Amitani, A. Igata, M. Matsumoto, and M. Tara.** 1986. HTLV-I associated myelopathy, a new clinical entity. Lancet **i:**1031–1032.
55. **Poiesz, B. J., F. W. Ruscetti, A. F. Gazdar, P. A. Bunn, J. D. Minna, and R. C. Gallo.** 1980. Detection and isolation of type C retrovirus particles from fresh and cultured lymphocytes of a patient with cutaneous T-cell lymphoma. Proc. Natl. Acad. Sci. USA **77:**7415–7419.
56. **Raghavan, A., R. L. Robison, J. McNabb, C. R. Miller, D. A. Williams, and P. R. Bohjanen.** 2001. HuA and tristetraprolin are induced following T cell activation and display distinct but overlapping RNA binding specificities. J. Biol. Chem. **276:**47958–47965.
57. **Rimsky, L., J. Hauber, M. Dukovich, M. H. Malim, A. Langlois, B. R. Cullen, and W. C. Greene.** 1988. Functional replacement of the HIV-1 rev protein by the HTLV-1 rex protein. Nature **335:**738–740.
58. **Simpson, R. M., T. M. Zhao, B. S. Hubbard, S. Sawasdikosol, and T. J. Kindt.** 1996. Experimental acute adult T cell leukemia-lymphoma is associated with thymic atrophy in human T cell leukemia virus type I infection. Lab. Investig. **74:**696–710.
59. **Stade, K., C. S. Ford, C. Guthrie, and K. Weis.** 1997. Exportin 1 (CRM1p) is an essential nuclear export factor. Cell **90:**1041–1050.
60. **Stein, G. M., U. Pfuller, M. Schietzel, and A. Bussing.** 2000. Expression of interleukin-4 in apoptotic cells: stimulation of the type-2 cytokine by different toxins in human peripheral blood mononuclear and tumor cells. Cytometry **41:**261–270.
61. **Stevenson, M., T. L. Stanwick, M. P. Dempsey, and C. A. Lamonica.** 1990. HIV-1 replication is controlled at the level of T cell activation and proviral integration. EMBO J. **9:**1551–1560.
62. **Taguchi, H., T. Sawada, A. Fukushima, J. Iwata, Y. Ohtsuki, H. Ueno, and I. Miyoshi.** 1993. Bilateral uveitis in a rabbit experimentally infected with human T-lymphotropic virus type I. Lab. Investig. **69:**336–339.
63. **Tanaka, Y., A. Yoshida, H. Tozawa, H. Shida, H. Nyunoya, and K. Shimotohno.** 1991. Production of a recombinant human T-cell leukemia virus type-I *trans*-activator (tax1) antigen and its utilization for generation of monoclonal antibodies against various epitopes on the tax1 antigen. Int. J. Cancer **48:**623–630.
64. **Tateno, M., N. Kondo, T. Itoh, T. Chubachi, T. Togashi, and T. Yoshiki.** 1984. Rat lymphoid cell lines with human T cell leukemia virus production. I. Biological and serological characterization. J. Exp. Med. **159:**1105–1116.
65. **Wang, G., R. Miskimins, and W. K. Miskimins.** 2000. Mimosine arrests cells in $G_1$ by enhancing the levels of p27 (Kip1). Exp. Cell Res. **254:**64–71.
66. **Werlen, G., E. Jacinto, Y. Xia, and M. Karin.** 1998. Calcineurin preferentially synergizes with PKC-θ to activate JNK and IL-2 promoter in T lymphocytes. EMBO J. **17:**3101–3111.
67. **Yoshida, M., M. Osame, K. Usuku, M. Matsumoto, and A. Igata.** 1987. Viruses detected in HTLV-I-associated myelopathy and adult T-cell leukaemia are identical on DNA blotting. Lancet **i:**1085–1086.
68. **Yoshida, M., T. Suzuki, J. Fujisawa, and H. Hirai.** 1995. HTLV-1 oncoprotein tax and cellular transcription factors. Curr. Top. Microbiol. Immunol. **193:**79–89.
69. **Zhang, X., Y. Hakata, Y. Tanaka, and H. Shida.** 2006. CRM1, an RNA transporter, is a major species-specific restriction factor of human T cell leukemia virus type 1 (HTLV-1) in rat cells. Microbes Infect. **8:**851–859.

Retrovirology

BioMed Central

Research

Open Access

# Activation and detection of HTLV-I Tax-specific CTLs by Epitope expressing Single-Chain Trimers of MHC Class I in a rat model

Takashi Ohashi*, Mika Nagai, Hiroyuki Okada, Ryo Takayanagi and Hisatoshi Shida

Address: Division of Molecular Virology, Institute for Genetic Medicine, Hokkaido University, Sapporo, 060-0815, Japan

Email: Takashi Ohashi* - ohashi-t@igm.hokudai.ac.jp; Mika Nagai - purefood@igm.hokudai.ac.jp; Hiroyuki Okada - hiro1230@igm.hokudai.ac.jp; Ryo Takayanagi - coffea-arabica@igm.hokudai.ac.jp; Hisatoshi Shida - hshida@igm.hokudai.ac.jp

* Corresponding author

Published: 8 October 2008

*Retrovirology* 2008, 5:90 doi:10.1186/1742-4690-5-90

Received: 22 July 2008
Accepted: 8 October 2008

This article is available from: http://www.retrovirology.com/content/5/1/90



## Abstract

**Background:** Human T cell leukemia virus type I (HTLV-I) causes adult T-cell leukemia (ATL) in infected individuals after a long incubation period. Immunological studies have suggested that insufficient host T cell response to HTLV-I is a potential risk factor for ATL. To understand the relationship between host T cell response and HTLV-I pathogenesis in a rat model system, we have developed an activation and detection system of HTLV-I Tax-specific cytotoxic T lymphocytes (CTLs) by Epitope expressing Single-Chain Trimers (SCTs) of MHC Class I.

**Results:** We have established expression vectors which encode SCTs of rat MHC-I (RT1.A$^l$) with Tax180-188 peptide. Human cell lines transfected with the established expression vectors were able to induce IFN-γ and TNF-α production by a Tax180-188-specific CTL line, 4O1/C8. We have further fused the C-terminus of SCTs to EGFP and established cells expressing SCT-EGFP fusion protein on the surface. By co-cultivating the cells with 4O1/C8, we have confirmed that the epitope-specific CTLs acquired SCT-EGFP fusion proteins and that these EGFP-possessed CTLs were detectable by flow cytometric analysis.

**Conclusion:** We have generated a SCT of rat MHC-I linked to Tax epitope peptide, which can be applicable for the induction of Tax-specific CTLs in rat model systems of HTLV-I infection. We have also established a detection system of Tax-specific CTLs by using cells expressing SCTs fused with EGFP. These systems will be useful tools in understanding the role of HTLV-I specific CTLs in HTLV-I pathogenesis.

## Background

Human T-cell leukemia virus type I (HTLV-I) is etiologically linked to adult T-cell leukemia (ATL) [1,2], a chronic progressive neurological disorder termed HTLV-I-associated myelopathy/tropical spastic paraparesis (HAM/TSP) [3,4], and various other human diseases [5-8]. ATL is a malignant lymphoproliferative disease affecting a subgroup of middle-aged HTLV-I carriers characterized by the presence of mature T cell phenotype [9]. HTLV-I genome contains a unique 3' region, designated as pX, which encodes the viral transactivator protein, Tax [10]. Because of its broad transactivation capabilities [11], it is specu-

lated that Tax plays a central role in HTLV-I associated immortalization and transformation of T cells, which may lead to the development of ATL.

Tax is also known as a major target protein recognized by cytotoxic T lymphocytes (CTL) of HTLV-I carriers [12]. It has been reported that the levels of HTLV-I-specific CTL are quite diverse among HTLV-I carriers and that ATL patients have impaired levels of HTLV-I specific CTLs in contrast to the high levels of CTL response in HTLV-I carriers with HAM/TSP [13-15]. In addition, it has been known that HTLV-I Tax-specific CTL response was strongly activated in ATL patients who acquired complete remission after hematopoietic stem cell transplantation [16]. Based on these observations, it is speculated that HTLV-I-specific immune response may contribute to repressing the growth of HTLV-I infected cells in the infected individuals and insufficient host T cell response against HTLV-I may be a risk factor for ATL.

To understand the mechanism of ATL development, it is very important to dissect the interplay between the virus-specific CTLs and HTLV-I infected T cells. We have previously established a rat model of ATL-like disease, which allows examination of the growth and spread of HTLV-I infected cells, as well assessment of the effects of immune T cells on the development of the disease [17,18]. By using this model system, we also reported the therapeutic effect of Tax-coding DNA or peptide against the disease [19,20]. For further analyzing the effects of Tax specific CTLs in the rat model, it is important to develop effective methods to activate Tax specific CTLs and to detect the virus-specific CTLs.

It has been reported that single chain trimers (SCTs) of MHC-I have the potential to efficiently stimulate and identify antigen specific T cells in both human and mouse systems [21,22]. In this system, all three components of MHC-I complexes, such as an antigen peptide, $\beta_2$-microgrobulin ($\beta_2$m), and MHC-I heavy chain are covalently attached with flexible linkers. By linking together the three components into a single chain chimeric protein, a complicated cellular machinery of normal antigen processing can be bypassed, leading to stable cell surface expression of MHC-I coupled with an antigenic peptide of interest. In addition, a new system has been established to identify virus-specific T cells using the acquisition mechanism of epitope/MHC complex by CD8 T cells through MHC/TCR interaction [23].

In this study, to establish an activation system of Tax-specific CTLs in our rat model system, we have generated a SCT of rat MHC-I linked to Tax epitope peptide. We have also established a detection system of Tax-specific CTLs by using cells expressing SCTs fused with EGFP. These newly established systems would be useful tools in understanding the role of HTLV-I specific CTLs in HTLV-I pathogenesis.

## Results

### *Production and functional capabilities of peptide-$\beta_2$m-RT1.A$^l$ fusion proteins*

To establish an activation system of Tax-specific CTLs using SCTs of rat MHC-I (RT1.A$^l$), we have constructed expression vectors as illustrated in Figure 1A. Tax180-188 epitope was previously identified as an RT1.A$^l$-restricted CTL epitope recognized by a Tax-specific CTL line [20]. As a negative control in this study, we have chosen a putative RT1.A$^l$-restricted epitope in the envelope of HIV-1 NL4-3 strain, NLEnv371-379, which was determined to have the same point as the Tax180-188 epitope scored by epitope prediction data via http://www.syfpeithi.de[24]. Since the linker length has been reported to influence the immune detection of SCTs in a mouse system [21], we have prepared SCTs with Tax180-188 or NLEnv 371–379 peptide linked by different lengths of spacers. We then performed an in vitro transfection experiment to assess the effects of SCTs for the activation of Tax-specific CTLs. The 293T cells were transfected with pEF/RT1Al, pEF/RT1AlSCNLEnv371S, pEF/RT1AlSCTax180S, or pEF/RT1AlSCTax180L. These transfected 293T cells were subsequently used to stimulate an RT1.A$^l$-restricted HTLV-I Tax180-188-specific CTL line, 4O1/C8. As shown in Figure 1B, 293T/RT1AlSCTax180S and 293T/RT1AlSCTax180L cells were able to induce IFN-γ secretion by 4O1/C8. Statistical analysis revealed a significant increase of IFN-γ production ($P = 0.02$) in 293T/RT1AlSCTax180L cells compared with 293T/RT1AlSCTax180S. In contrast, 293T/RT1Al, 293T/RT1AlSCNLEnv371S, and nontransfected 293T cells induced little IFN-γ secretion by the Tax-specific CTLs. We have also confirmed the induction of TNF-α production by these vectors, although there was no significant difference observed between 293T/RT1AlSCTax180L and 293T/RT1AlSCTax180S cells (Figure 1D). These results suggested that Tax180-188/$\beta_2$m/RT1.A$^l$ SCTs were efficiently expressed on the cell surface of the transfected cells and were recognized by the epitope-specific CTLs.

### *Establishment of MOLT-4 cells stably expressing SCTs of RT1.A$^l$*

To examine the effects of rat SCTs expressed on human cells and the influence of linker length on the activation of CTLs in more detail, we have introduced the expression vectors into MOLT-4 cells and established the cells stably expressing SCTs of RT1.A$^l$ with the different linker length. After selection by G418 and cloning, FACS analysis was performed to determine the expression level of RT1.A$^l$ on MOLT-4 cells. As shown in Figure 2A, equivalent levels of SCT expression were confirmed on the surface of MOLT-4/RT1AlSCTax180S and MOLT-4/RT1AlSCTax180L cells,

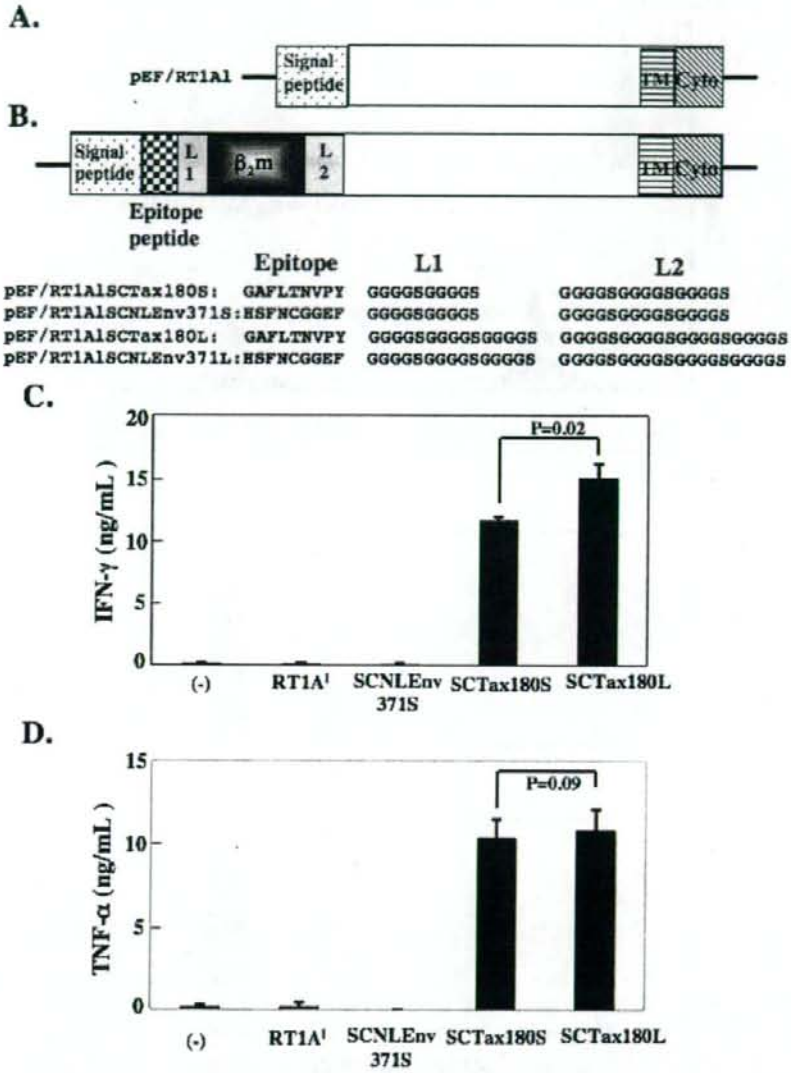


**Figure 1**

**Activation of Tax-specific CTLs by 293T cells expressing SCTs with Tax 180–188 epitope.** (A) Diagram of full-length rat MHC-I (RT1.A$^l$). (B) Diagram of SCTs encoding Tax180-188 or NLEnv371-379 linked to $\beta_2$m and RT1.A$^l$ molecules with different lengths of linkers. L1, linker 1; TM, transmembrane region; Cyto, cytoplasmic region. (C and D) The 293T cells were either untreated or transfected with pEF/RT1Al, pEF/RT1AlSCNLEnv371S, pEF/RT1AlSCTax180S, or pEF/RT1AlSCTax180L. The 293T cells were then incubated with a Tax-specific CD8+ T cell line, 4O1/C8. Production of IFN-γ (C) and TNF-α (D) in the supernatants was measured by ELISA after 24 hours of culture. The data represent the mean ± the SD of triplicate wells. Similar results were obtained in two independent experiments.

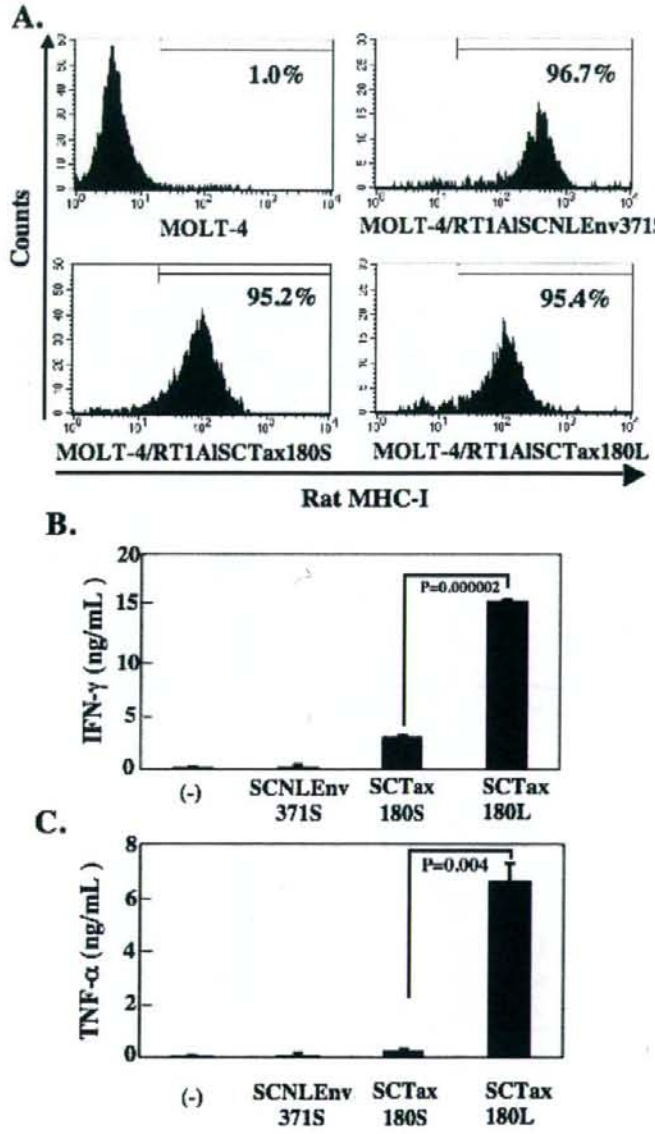


**Figure 2**
**Establishment of MOLT-4 cells stably expressing SCTs of RT1.Al.** (A) MOLT-4 cells were transfected with various SCT expression vectors. After selection by G418 and cloning, flow cytometric analysis was performed to determine the expression level of RT1.Al on MOLT-4 cells. The percentage of RT1.Al-positive cells is indicated in each part. (B and C) The MOLT-4 cells expression with indicated SCTs were incubated with a Tax-specific CD8+ T cell line, 4O1/C8. Production of IFN-γ (B) and TNF-α (C) in the supernatants was then measured by ELISA after 24 hours of culture. The data represent the mean ± the SD of triplicate wells. Similar results were obtained in two independent experiments.

whereas we detected higher mean fluorescence intensity (MFI) in MOLT-4/RT1AlSCNLEnv371S compared with the other 2 SCT-transfected cells. These SCTs expressing MOLT-4 cells were subsequently used to stimulate 4O1/C8 cells. As shown in Figure 2B and 2C, MOLT-4/RT1AlSCTax180S and MOLT-4/RT1AlSCTax180L cells were able to induce both IFN-γ and TNF-α secretions by 4O1/C8. MOLT-4/RT1AlSCTax180L induced significantly higher levels of IFN-γ and TNF-α than those induced by MOLT-4/RT1AlSCTax180S, suggesting that the SCT with the longer linker has a higher affinity to the epitope-specific TCR. In contrast, MOLT-4/RT1AlSCNLEnv371S cells induced little IFN-γ and TNF-α secretion by the Tax-specific CTLs, despite the higher expression of SCTs. Parental MOLT-4 cells did not stimulate the cytokine secretion, either. These results indicated that the SCTs with longer linkers have the advantage to efficiently stimulate the epitope-specific CTLs and suggested that the longer form would be suitable for further application of immunological study.

### *Inhibitory effects of SCTs expressing Tax180-188 on the growth of Tax-specific CTLs*

We next examined whether the SCTs could induce the expansion of epitope-specific CTLs in vitro. A series of SCT-expressing MOLT-4 cell lines were fixed with formalin and then used as stimulators for 4O1/C8. An HTLV-I infected syngeneic rat cell line, FPM1.BP, was also used as a stimulator, because it has been used to stimulate 4O1/C8 cells and was thus known to induce the proliferation of the CTLs. After 3 days of mixed culture, the growth of 4O1/C8 was evaluated. As shown in Figure 3A, FPM1.BP cells significantly enhanced the growth of 4O1/C8 as compared with untransfected MOLT-4 cells. In contrast, MOLT-4 cells expressing SCTs with Tax180 did not induce the proliferation of 4O1/C8, but significantly inhibited the growth of the CTLs. We detected stronger growth inhibition in MOLT-4 cells with longer linkers than those with shorter linkers. The expression of SCTs with NLEnv371 on MOLT-4 cells caused no influence on the growth of 4O1/C8. We also assessed the IFN-γ production in the mixed culture and confirmed the significantly high level of the cytokine in the culture of FPM1.BP. It was of note that IFN-γ production was inversely correlated with the growth of 4O1/C8 among the mixed cultures of MOLT-4 cells with different SCTs, suggesting that observed growth inhibition was due to the activation induced cell death (AICD). Thus, we further investigated the apoptotic status of 4O1/C8 by Annexin V staining. As shown in Figure 3C, we observed the increase of Annexin V positive cells after mixed culture with MOLT-4 cells expressing SCTs with Tax180, but not with those expressing SCTs with NLEnv371S. As correlated with the growth inhibition, the SCTs with longer linker induced higher rate of apoptosis in 4O1/C8 cells than those with shorter linker did. It is of note that a much higher level of apoptosis was observed in the mixed culture of FPM1.BP cells, indicating that FPM1.BP was able to promote the growth of 4O1/C8 even though it induced a higher level of AICD at the same time. To understand the mechanism of enhanced proliferation induced by FPM1.BP, we have assessed the IL-2 concentration in the mixed culture and found that production of the T cell-stimulatory cytokine was dramatically enhanced by FPM1.BP cells (Figure 3D). These results suggested that the growth inhibition by SCTs with Tax resulted from both an enhanced level of AICD and a reduced activation of proliferation signal(s) including IL-2 pathways, which FPM1.BP cells were able to stimulate.

### *Detection of Tax-specific CTLs by SCTs fused with EGFP*

To establish a detection system of Tax-specific CTLs, the single chain peptide-RT1.A$^l$ construct was then fused at its C-terminal end to EGFP as illustrated in Figure 4A. We have prepared two constructs with covalently linked Tax180-188 or NLEnv371-379 peptides with longer linkers, which were designated as pEF/RT1AlSCTax180L-EGFP and pEF/RT1AlSCNLEnv371L-EGFP, respectively. We have also generated a construct, which can express only RT1.A$^l$ fused at its C-terminus to EGFP (pEF/RT1Al-EGFP). These vectors were transfected into 293T cells to express fusion proteins on the surface. To determine whether SCTs with EGFP are properly expressed on the surface of 293T cells, we have incubated the transfected 293T cells with 4O1/C8 and then assessed the IFN-γ and TNF-α production in the mixed culture. As shown in Figure 4B and 4C, neither 4O1/C8 cells mixed with parental 293T nor those with 293T/RT1Al-EGFP produced detectable levels of IFN-γ and TNF-α. When we pulsed the 293T/RT1Al-EGFP with 10 μM of Tax180-188 peptides, but not with NLEnv371-379 peptides, for 30 min before co-cultivation, we clearly detected the increase of IFN-γ and TNF-α production in the culture. The 293T cells expressing RT1AlSCTax180L-EGFP also induced IFN-γ and TNF-α production, but those expressing RT1AlSCNLEnv371L-EGFP did not. These results indicated that RT1.A$^l$-EGFP fusion proteins with epitope peptides were efficiently recognized by Tax-specific CTLs.

To determine whether SCTs with EGFP can be acquired by antigen-specific CTLs, we incubated the transfected 293T cells together with 4O1/C8 cells or another CD8+ syngeneic T cell line, G14, which is not specific to Tax 180-188. As shown in Figure 5A, more than 60% of 4O1/C8 cells appeared to be positive for EGFP after mixed culture with 293T/RT1AlSCTax180L-EGFP cells for 1 hour, but not with 293T/RT1AlSCNLEnv371L-EGFP. In contrast, we were unable to detect G14 cells acquiring EGFP after mixed culture with 293T/RT1AlSCTax180L-EGFP. To confirm the acquisition of SCT-EGFP fusion proteins by 4O1/C8, we examined the cells by confocal microscopy. As

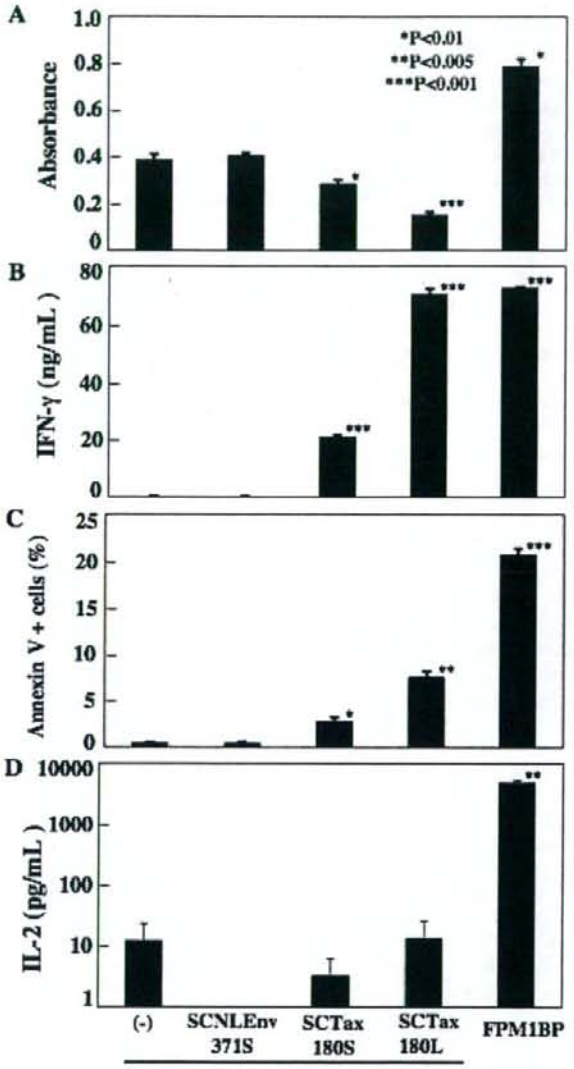


**Figure 3**

**(A) Inhibitory effects of SCTs expressing Tax180-188 on the growth of Tax-specific CTLs.** An HTLV-I infected syngeneic rat cell line, FPM1.BP or various MOLT-4 cells were fixed with formalin and were then mixed with 4O1/C8. After 3 days of mixed culture, the growth of 4O1/C8 was evaluated using cell counting kit-8. (B) Production of IFN-γ in the culture supernatants was measured by ELISA after 3 days of mixed culture. (C) Apoptotic status of 4O1/C8 was evaluated by staining with Annexin V-FITC and anti-rat CD8 Ab-PE. (D) Production of IL-2 in the culture supernatants was measured by ELISA after 2 days of mixed culture. *P < 0.01, **P < 0.05, and ***P < 0.001 compared to the mixed culture with parental MOLT-4 cells. The data represent the mean ± the SD of triplicate wells. Similar results were obtained in two independent experiments.

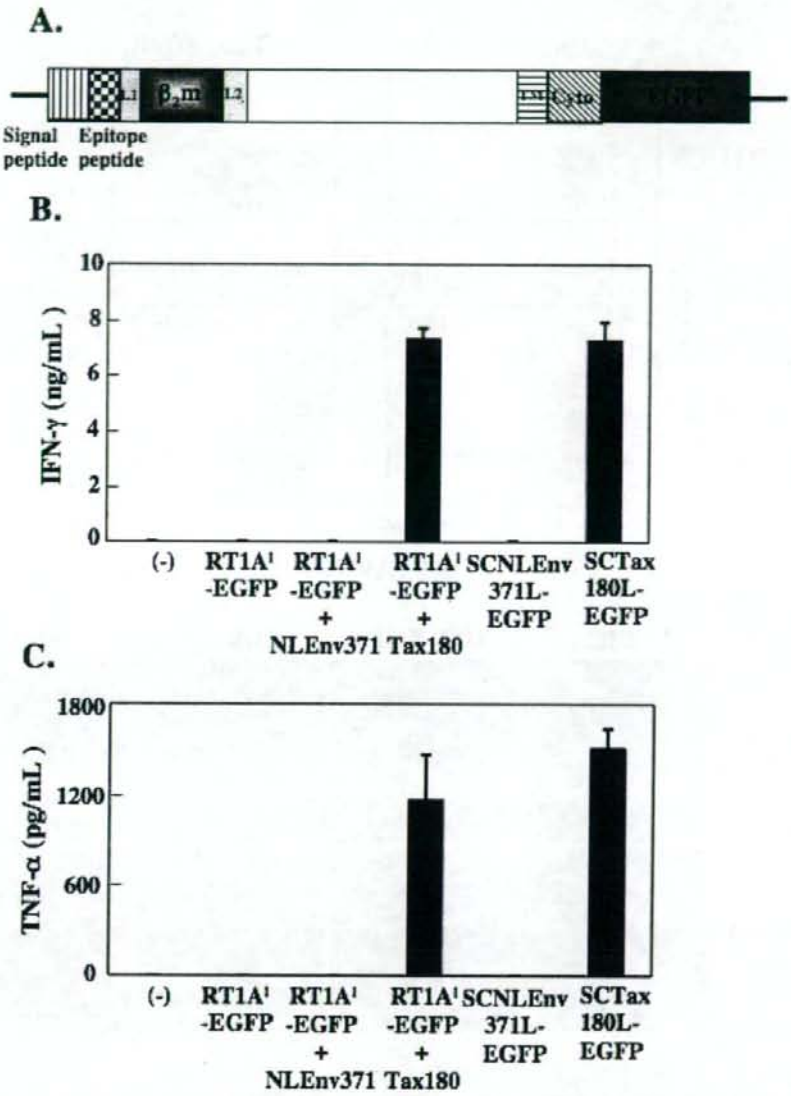


**Figure 4**

**Expression of SCTs of RT1.A¹ fused with EGFP. (A) Diagram of SCTs of RT1.A¹ fused at its C-terminal end to EGFP.** (B and C) The 293T cells were either untreated or transfected with pEF/RT1AI-EGFP, pEF/RT1AISCNLEnv371L-EGFP, or pEF/RT1AISCTax180L-EGFP. After 48 hours of transfection, the 293T cells were incubated with 4O1/C8 cells for 24 hours. Production of IFN-γ (B) and TNF-α (C) in the supernatants was measured by ELISA. For 293T/RT1AI-EGFP cells, NLEnv371-379 or Tax180-188 peptides were pulsed for 30 min before the mixed culture with 4O1/C8. The data represent the mean ± the SD of triplicate wells. Similar results were obtained in two independent experiments.

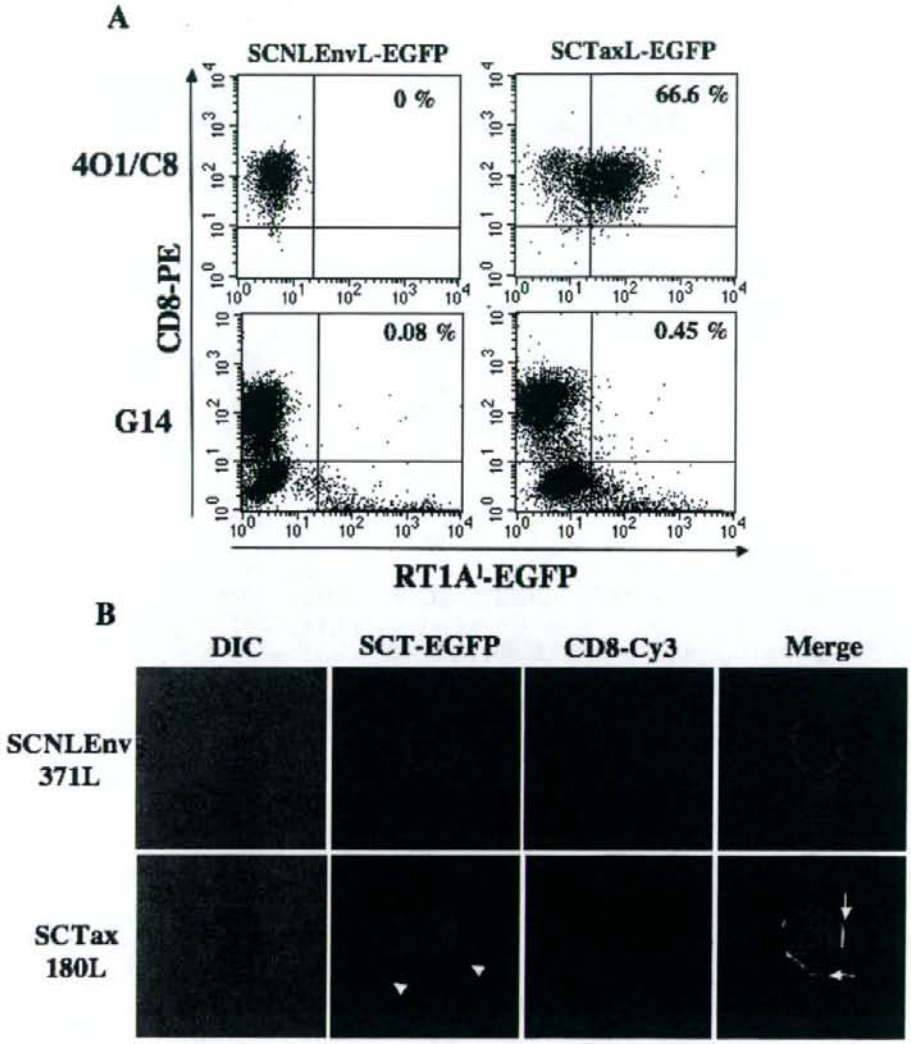


**Figure 5**
**Detection of Tax-specific CTLs by SCTs fused with EGFP. (A) The 293T cells transfected with pEF/RT1AlSCNLEnv371L-EGFP or pEF/RT1AlSCTax180L-EGFP were incubated with 4O1/C8 or control G14 cells.** After 1 hour of mixed culture, cells were stained with PE-conjugated anti-rat CD8 antibody and EGFP expression on CD8+ cells were assessed by flow cytometric analysis. (B) Cells in the mixed culture of 4O1/C8 and EGFP-expressing 293T cells were attached on slide glasses by centrifugation, fixed with 4% paraformaldehyde for 15 min at room temperature and then stained with an anti-rat CD8 antibody in combination with a Cy3-conjugated goat anti-mouse IgG (H+L) antibody. Fluorescence and differential interference contrast (DIC) images were obtained with a confocal microscope system and a pair of GFP and CD8 images was overlaid (merge). Arrowheads indicate SCT-EGFP in 4O1/C8 cells. Arrows indicate co-localization of SCT-EGFP and CD8 at the contact site. Similar results were obtained in two independent experiments.

shown in Figure 5B, SCT-EGFP with Tax180 molecules formed large clusters at 4O1/C8-293T contact sites (arrows) and appeared in 4O1/C8 cells (arrowheads) after 1 hour of mixed culture. In contrast, we were unable to detect the acquisition of EGFP fusion proteins by the CTLs after the mixed culture with 293T/RT1AlSCNLEnv371L-EGFP. Thus, RT1.AlSCTaxL-EGFP fusion proteins were specifically acquired by the epitope specific CTLs.

#### *Detection of Tax-specific CTLs in splenocytes derived from HTLV-I infected rats*

By using SCTs fused with EGFP, we have tried to detect Tax-specific CTLs in rats infected with HTLV-I. To prepare HTLV-I infected rats, we have intraperitoneally inoculated F344 rats with $1 \times 10^7$ FPM1.BP cells 3 times. One week after the last inoculation, splenocytes were purified and subjected to FACS analysis to detect Tax-specific CTLs. At first, we tried to detect the CTLs in unstimulated splenocytes, but have so far failed in the attempt, probably because of the low frequency of Tax180-188-specific CTLs in HTLV-I infected rats prepared in this study (data not shown). Thus, we have stimulated the splenocytes in vitro with formalin-fixed FPM1.BP cells twice with 1-week intervals and examined the frequency of Tax180-188-specific CTLs 1 week after each stimulation. As shown in Figure 6A, SCT-EGFP staining of splenocytes from an HTLV-I-infected rat revealed that 11.0 ± 6.5% of CD8+ cells were specifically bound to the SCT-EGFP with Tax180 after the first stimulation. Also, the second stimulation of splenocytes with FPM1.BP expanded the RT1.AlSCTaxL-EGFP positive cell population to 16.5 ± 1.4% of CD8+ cells. In contrast, we were unable to detect a significant level of Tax180-188 CTL induction in the splenocytes derived from a PBS-inoculated uninfected rat. The SCT-EGFP with NLEnv371 did not bind to CD8+ cells derived from an HTLV-I-infected or uninfected control rat. To assess the comparability of the SCT-EGFP staining to other antigen-specific T-cell screening systems, we have stimulated the splenocytes with Tax180-188 or NLEnv371-379 peptides and examined IFN-γ production in the culture. As shown in Figure 6B, stimulation with Tax180-188 peptides induced a significant level of IFN-γ production by splenocytes from an HTLV-I-infected rat after first stimulation. In splenocytes that received the second stimulation, we have detected the enhanced production of IFN-γ after addition of Tax180-188 peptides in an HTLV-I-infected rat, but not in an uninfected control rat. This induction of IFN-γ production was specific to Tax180-188 peptides, because NLEnv371-379 peptides failed to induce a significant level of the cytokine production. Thus, these results indicated that RT1.AlSCTaxL-EGFP fusion proteins were able to detect Tax180-188 specific CTLs in primary splenocytes derived from an HTLV-I-infected rat and that the detection of the epitope specific CTLs by SCT-EGFP fusion proteins was comparable to the assessment of epitope specific production of IFN-γ.

## Discussion

In this study, by using epitope expressing SCTs of rat MHC Class I, we have developed an activation and detection system of HTLV-I Tax-specific CTLs which can be applicable for analyzing CTL responses in a rat model system of HTLV-I infection. The SCT system has been developed in mouse and human MHC-I with its corresponding epitopes [25,26], but not in rat MHC-I. Based on the information previously reported on the mouse system [21], we have designed expression vectors for SCTs of rat RT1.A$^l$ and successfully obtained the constructs which can activate epitope specific CTLs in vitro. We have further developed the CTL detection system by combining the SCT complex with EGFP, which should be transferred to epitope specific CTLs as previously reported [23]. Because of the poor availability of MHC-I tetramers in rats, development of this system will provide various benefits in analyzing the role of CTLs in a variety of disease models in rats.

The Tax180-188 epitope used in this study was previously identified by epitope mapping analysis and was actually confirmed to be one of the major epitopes presented by RT1.A$^l$ in F344 rats infected with HTLV-I or immunized with Tax protein [20,27]. On the other hand, NLEnv371-379 epitope was predicted by "SYFPEITHI epitope prediction algorithm" [24] and was given 27 points in the scoring system. Since Tax180-188 was given the same points as NLEnv371-379 scored, it would be reasonable to assume that NLEnv371-379 epitope was equivalently presented by RT1.A$^l$ in our present experiments. Nevertheless, only SCTs with Tax180, but not with NLEnv371 can recognize and activate Tax180-188 specific CTLs. Moreover, SCTs with Tax180 did not recognize another CD8+ T cell line, G14, which is not specific to Tax180-188. These results indicated that the SCTs of RT1.A$^l$ engineered in the present study appropriately presented the Tax epitope to the corresponding CTLs. However, it is still necessary to establish new CTL lines with different epitope specificities for further confirming the epitope specificity of SCTs used in this study. In addition, it is important to identify new CTL epitopes in rat model of HTLV-I infection for better understanding of the relationship between diversity of HTLV-I-specific CTLs and the virus-related diseases. Especially, recently identified HTLV-I basic leucine zipper factor (HBZ) is the most important factor to be analyzed as a CTL target because of its possible involvement in ATL development [28]. The SCT system together with RT1.A$^l$-EGFP complex should be applicable for the search of new epitopes in F344 rats. Indeed, Tomaru et. al successfully detected new CD8+ T cell epitope from the envelope

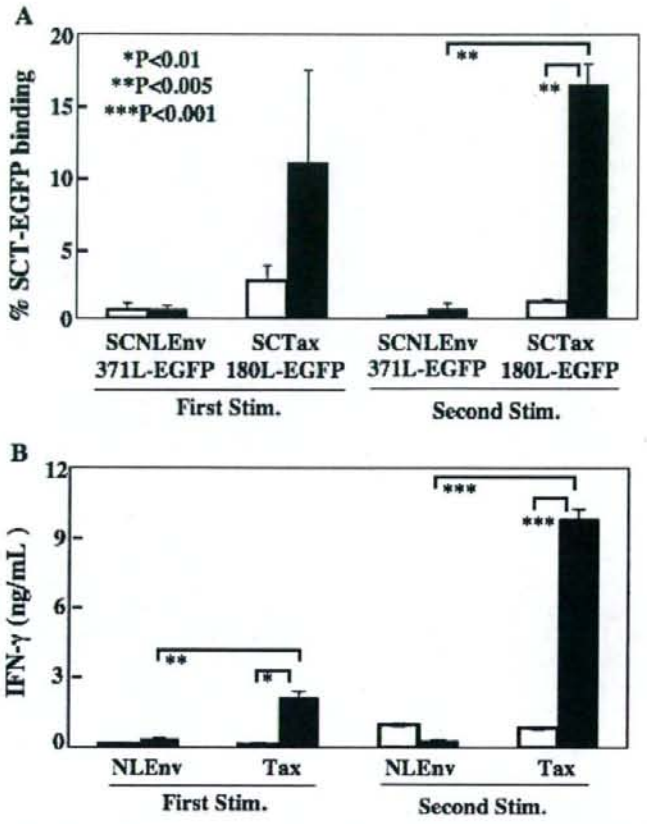


**Figure 6** *(see previous page)*
**Detection of Tax-specific CTLs in primary splenocytes stimulated with FPM1.BP cells in vitro (A) Splenocytes were isolated from an HTLV-I infected (•) or uninfected control (□) rat and then stimulated with formalin-fixed FPM1.BP cells twice with 1-week interval.** One week after the first or second stimulation, splenocytes were purified and then incubated with the 293T cells transfected with pEF/RT1AlSCNLEnv371L-EGFP or pEF/RT1AlSCTax180L-EGFP. One hour after the mixed culture, cells were stained with PE-conjugated anti-rat CD8 antibody and EGFP expression on CD8+ cells were assessed by flow cytometric analysis. The percent CD8+ cells that stain positively with each SCT-EGFP were shown. The data represent the mean ± the SD of triplicate analyses. (B) One week after the first or second stimulation, splenocytes were purified and then stimulated with 10 μM of Tax180-188 or NLEnv371-379 peptides for 48 hours. Production of IFN-γ in the culture supernatants was measured by ELISA. The data represent the mean ± the SD of triplicate wells.

region of HTLV-I using HLA-A2-EGFP fusion proteins [23].

MOLT-4/RT1AlSCTax180L cells induced the production of IFN-γ by 4O1/C8 CTLs. However, the activated 4O1/C8 cells failed to proliferate, but rather tended to decrease the number in the mixed culture (Figure 3). This is in dramatic contrast to the results observed in the mixed culture of 4O1/C8 with FPM1.BP, wherein both IFN-γ production and cell proliferation were enhanced. Although the exact mechanism of this difference is not clear, our results suggest that the failure of CTL expansion was due to the enhanced apoptosis induced by RT1AlSCTax180L. In this regard, it has been reported that the presence of CD4+